

Magnetic alteration of entanglement in two-electron quantum dots

N. S. Simonović¹ and R.G. Nazmitdinov^{2,3}

¹*Institute of Physics, University of Belgrade, P.O. Box 57, 11001 Belgrade, Serbia*

²*Departament de Física, Universitat de les Illes Balears, E-07122 Palma de Mallorca, Spain*

³*Bogoliubov Laboratory of Theoretical Physics, Joint Institute for Nuclear Research, 141980 Dubna, Russia*

Quantum entanglement is analyzed thoroughly in the case of the ground and lowest states of two-electron axially symmetric quantum dots under a perpendicular magnetic field. The individual-particle and the center-of-mass representations are used to study the entanglement variation at the transition from interacting to noninteracting particle regimes. The mechanism of symmetry breaking due to the interaction, that results in the states with symmetries related to the later representation only, being entangled even at the vanishing interaction, is discussed. The analytical expression for the entanglement measure based on the linear entropy is derived in the limit of noninteracting electrons. It reproduces remarkably well the numerical results for the lowest states with the magnetic quantum number $M \geq 2$ in the interacting regime. It is found that the entanglement of the ground state is a discontinuous function of the field strength. A method to estimate the entanglement of the ground state, characterized by the quantum number M , with the aid of the magnetic field dependence of the addition energy is proposed.

PACS numbers: 03.67.Bg, 03.67.Mn, 73.21.La

I. INTRODUCTION

Quantum entanglement and its implications such as quantum teleportation, quantum cryptography, and quantum computation, to name just a few (for a review see [1–3]), are the subject of intense research efforts in recent years. Apart from possible practical applications, these research lines provide a deeper understanding of the fundamental aspects of quantum correlations in many-body systems. This issue is currently the focus of an increasing research activity, establishing new connections between quantum information theory and quantum correlations in atomic, molecular and condensed matter physics [4, 5].

Among suitable systems, capable of demonstrating a relationship between quantum entanglement and quantum correlations, are quantum dots (QDs). They offer one of the perspective experimental platforms for quantum communications in solid-state environment [6] and allow the study of various aspects of quantum correlations with a high accuracy [7–9]. Indeed, control of QD spectra by gates and an external magnetic field provides an efficient way to create a single-electron ground state manifold with well-defined spin states. According to a general wisdom, spin degrees of freedom in QDs are promising candidates for quantum information processing (see, e.g., [10, 11]). At the same time, quantum communication research considers photons as flying qubits that carry quantum information over long distances. QDs appear as remarkable candidates to realize the interface between stationary qubits and flying photonic qubits. The optical excitation spectra of QDs exhibits strong correlations between the initial electron state and light polarization. This leads to the possibility to explore QD spin-photon entanglement, that nowadays emerges in the fast developing field of coherent optical manipulation of spin states in a solid-state environment

(for a review see [12]).

To operate efficiently by stationary qubits it is necessary to deepen our understanding of various aspects of quantum correlations brought about by the electron-electron interaction, an effective confining potential, external fields, and the degree of entanglement in QDs. Besides computational problems for many-body quantum systems, one has to address to the problem of measuring entanglement for indistinguishable particles. In other words, one has to discriminate entanglement from correlations due to the statistics of indistinguishable particles [13–15]. In spite of this difficulty, bipartite entanglement has been investigated in a number of systems of physical interest with the aid of various numerical approaches at zero magnetic field. In particular, the connection between entanglement and correlation energy has been studied in the context of a two-electron artificial atom [16]. The amount of entanglement of the ground state and of the first few excited states of helium was assessed by using high-quality state-of-the-art wavefunctions [17]. Benenti et al. [18] used a configuration-interaction variational method to compute the von Neumann and the linear entropy for several low-energy singlet and triplet eigenstates of helium. Lin et al. [19] computed the spatial quantum entanglement of helium-like ions by means of spline techniques. Various types of wave functions have been used to increase the numerical accuracy of the entanglement measures of helium-like atoms with a few electrons [20–22]. Also, the entanglement properties of bound states in the two-electron Moshinsky model [23] and a solvable model of two-electron parabolic quantum dot [24] were investigated.

Two-electron QDs being realistic non-trivial systems are particularly attractive for a detailed analysis of quantum correlations (for a review see [25]). In contrast to many electron QDs, their eigenstates can be obtained very accurately, or in some cases exactly. The same con-

conveniences also hold while calculating appropriate entanglement measures. The spatial entanglement measures have been used to test the validity of approximations of the density-functional theory for Hook's atom [26]. It represents a possible model for describing two electrons trapped in a quantum dot. Further, it was found that the entanglement of the singlet state increases with the increase of the dimension of the Hook's system [27]. It was shown that the anisotropy of the confining potential of two-dimensional two-electron QD drastically influences the entanglement properties in a strong correlation regime [28]. The entanglement (linear entropy) has been calculated to trace the transition from bound to continuum states in two-electron QDs [29]. The study of a two-electron QD by means of entanglement witness provided new aspects in the ongoing discussion about the origin of Hund's rules in atoms [30]. It was shown that the presence of the donor-impurity has little impact on the entanglement in two-electron QDs in the regime of formation of the Wigner molecule [31].

We recall that all these studies are mostly focused on the interconnection between quantum correlations and various measures of entanglement at zero magnetic field, with a different degree of numerical accuracy. In this paper we will analyze this relationship in the lowest states of two-electron QDs, that are evolving to the ground states in different intervals of the magnetic field strength. To this aim we will present a numerical and an analytical approach that describes remarkably well the numerical results. Special attention is paid to the study of quantum correlations and the entanglement in the limiting case of noninteracting electrons in order to elucidate the impact of the electron-electron interaction and/or the magnetic field. Preliminary results of our analysis have been presented in [32, 33], where the influence of the magnetic field on the entanglement of the singlet $m = 0$ states only has been investigated.

The structure of the paper is as follows. In Sec. II we set up the model for axially symmetric two-electron QDs in a magnetic field directed along the symmetry axis, analyze integrals of motion and symmetries in the cases with and without the electron-electron (V_C) interaction, and introduce appropriate basis sets. We also consider here entanglement measures for two-electron states. In Secs. III and IV, we analyze the orbital properties of the lowest eigenstates in the limit $V_C \rightarrow 0$, in the individual particle and the center-of-mass representations, respectively. In Sec. IV we consider also the dependence of the entanglement of QD lowest states on the strengths of the Coulomb interaction between electrons as well as on the magnetic field. Sec. V establishes the transformation of one representation to another one. The entanglement of the ground state, particularly in the light of the so-called singlet-triplet transitions, is analyzed in Sec. VI. In Sec. VII we describe how to estimate the entanglement at different field strengths by means of experimental observations. Main conclusions are summarized in Sec. VIII. In Appendices A–E we present some technical details of

our analysis.

II. THE MODEL

A. The Hamiltonian

Our analysis is based on the Hamiltonian

$$H_{\text{tot}} = \sum_{i=1}^2 H_i + V_C + H_S = H + H_S, \quad (1)$$

where

$$H_i = \frac{1}{2m^*} (\mathbf{p}_i - e\mathbf{A}_i)^2 + U(\mathbf{r}_i), \quad (2)$$

The term $V_C = \lambda/|\mathbf{r}_1 - \mathbf{r}_2|$ with $\lambda = e^2/4\pi\epsilon_0\epsilon_r$ describes the Coulomb interaction between electrons. The constants m^* , e , ϵ_0 and ϵ_r are the effective electron mass, unit charge, vacuum and relative dielectric constants of a semiconductor, respectively. In the expressions above \mathbf{r}_i and \mathbf{p}_i ($i = 1, 2$) are the positions and momenta of the electrons, respectively, and $U(\mathbf{r}_i)$ is the i -th electron confining potential. The orbital and spin degrees of freedom (the terms H and H_S in Eq. (1)) are fully decoupled in our model, since we neglect the spin-orbit interaction

The influence of the magnetic field (we set the z -axis along the vector \mathbf{B}) on the electron orbital motion is introduced through the vector potential with gauge $\mathbf{A} = \frac{1}{2}\mathbf{B} \times \mathbf{r} = \frac{1}{2}B(-y, x, 0)$. The term $H_S = g^*\mu_B B S_z/\hbar$ in (1) describes the interaction of the (total) spin $\mathbf{S} = \mathbf{s}_1 + \mathbf{s}_2$ with the magnetic field. Here S_z is the z -projection of the total spin, g^* is the effective Landé factor, and $\mu_B = |e|\hbar/2m_e$ is the Bohr magneton.

For axially symmetric QDs (with z -symmetry axis) the confining potential is quite well approximated by the parabolic model [25]. We consider the form $U(\mathbf{r}) = \frac{1}{2}m^*u(\omega_0; \mathbf{r})$, where

$$u(\omega_0; \mathbf{r}) = \omega_0^2(x^2 + y^2) + \omega_z^2 z^2. \quad (3)$$

Here $\hbar\omega_0$ and $\hbar\omega_z$ are the energy scales of the confinement in the xy -plane (lateral confinement) and in the z -direction (vertical confinement), respectively. We also introduce the characteristic lengths of the lateral and vertical confinements, $\ell_0 = \sqrt{\hbar/m^*\omega_0}$ and $\ell_z = \sqrt{\hbar/m^*\omega_z}$, respectively. In the extremely anisotropic case $\omega_z \gg \omega_0$ one has $\langle z^2 \rangle \ll \langle x^2 + y^2 \rangle$, and the Coulomb term V_C reduces to the form $\lambda/[(x_1 - x_2)^2 + (y_1 - y_2)^2]^{1/2}$. As a consequence, the motions in the xy -plane and along the z -axis are practically decoupled (see discussion in [34]). In this case the 2D (planar) model is a good approximation. This is due to the fact that electrons perform only fast harmonic oscillations in the z -direction. As a result, the states with the lowest energy of z -component ($2 \times \hbar\omega_z/2$) are occupied only.

Applying the above given gauge condition, we have for the single-electron Hamiltonians

$$H_i = \frac{\mathbf{p}_i^2}{2m^*} + \frac{1}{2}m^*u(\Omega; \mathbf{r}_i) - \omega_L l_z^{(i)}, \quad (4)$$

where $\omega_L = eB/2m^*$ is the Larmor frequency and $\Omega = (\omega_0^2 + \omega_L^2)^{1/2}$ is the effective lateral confinement frequency that depends through the frequency ω_L on the magnetic field. The operator $l_z^{(i)}$ is the z -projection of the angular momentum of the i -th electron. Evidently, in the approximation of noninteracting electrons ($V_C = 0$) the single-electron energies and orbital momenta are integrals of motion. At $V_C \neq 0$ the quantities related to the electron collective dynamics are conserved only (see below).

By introducing the center of mass (c.m.) $\mathbf{R} = \frac{1}{2}(\mathbf{r}_1 + \mathbf{r}_2)$ and relative $\mathbf{r}_{12} = \mathbf{r}_1 - \mathbf{r}_2$ coordinates, the orbital part of Hamiltonian (1) separates into the c.m. and relative motion terms, $H = H_{\text{c.m.}} + H_{\text{rel}}$ (see details in [25]), in agreement with the Kohn theorem [35]. The c.m. term has the form

$$H_{\text{c.m.}} = \frac{\mathbf{P}^2}{2\mathcal{M}} + \frac{1}{2}\mathcal{M}u(\Omega; \mathbf{R}) - \omega_L l_z^{(\text{c.m.})}, \quad (5)$$

where $\mathcal{M} = 2m^*$ is the total mass, and $l_z^{(\text{c.m.})}$ is the z -projection of the c.m. angular momentum. The relative motion term includes the Coulomb interaction between electrons

$$H_{\text{rel}} = \frac{\mathbf{p}_{12}^2}{2\mu} + \frac{1}{2}\mu u(\Omega; \mathbf{r}_{12}) - \omega_L l_z^{(\text{rel})} + \frac{\lambda}{r_{12}} = H_{\text{rel}}^{(0)} + V_C. \quad (6)$$

Here $\mu = m^*/2$ is the reduced mass, and $l_z^{(\text{rel})}$ is the z -projection of the angular momentum for the relative motion. Both projections $l_z^{(\text{c.m.})}$, $l_z^{(\text{rel})}$, are integrals of motion due to the axial symmetry of the system.

Finally, it should be mentioned that the Hamiltonian H and the corresponding equations of motion are invariant under the scaling transformations $\mathbf{r}_i \rightarrow \mathbf{r}_i/\ell_0$, $\mathbf{p}_i \rightarrow \mathbf{p}_i\ell_0/\hbar$ and $E \rightarrow E/\hbar\omega_0$. As a consequence, the Hamiltonian H expressed in scaled variables is invariant under the simultaneous variations of the QD parameters that keep constant the ratio ω_z/ω_0 and the scaled strength of the Coulomb interaction $\lambda/(\hbar\omega_0\ell_0) \equiv \ell_0/a^* = R_W$ (the so-called Wigner parameter). Here, $a^* = \hbar^2/\lambda m^*$ is the effective Bohr radius. In other words, the whole class of axially symmetric QDs can be covered by varying only these two parameters, and the additional parameter ω_L/ω_0 if $B \neq 0$. In particular, we will use the value $R_W = 2$ that corresponds to a typical GaAs QD ($m^* = 0.067 m_e$, $\varepsilon_r \approx 12$, $\hbar\omega_0 = 3.165 \text{ meV}$.)

B. Integrals of motion and symmetries

As discussed above, the orbital and the spin degrees of freedom are decoupled in our system. As a result, the eigenstates of Hamiltonian (1) take the form

$$\Psi = \psi(\mathbf{r}_1, \mathbf{r}_2)\chi(\sigma_1, \sigma_2), \quad (7)$$

where ψ and χ are the orbital and spin parts, respectively. The spins of individual electrons and their z -projections as well as the total spin and its z -projection are the integrals of motion. We have two alternative sets of spin quantum numbers: $\{s_1, s_2, m_{s1}, m_{s2}\}$ and $\{s_1, s_2, S, M_S\}$. Here we choose the second set that provides a definite exchange symmetry of two-electron states.

The orbital motion is characterized by several integrals of motion. The corresponding operators $H_{\text{c.m.}}$, $l_z^{(\text{c.m.})}$, H_{rel} , $l_z^{(\text{rel})}$ (and $H_z^{(\text{c.m.})}$ in the 3D case) commute with H , and also mutually. Since in the 2D case there are four independent integrals of motion that are in involution, the 2D model (it has four orbital degrees of freedom) is fully integrable. Therefore, these four operators define a complete set of commuting observables (CSCO). In the 3D case the system is, however, generally non-integrable at $V_C \neq 0$, excluding some special cases [36–38]. Evidently, we have to use as basis states those that are defined at $V_C = 0$.

For noninteracting electrons there are two appropriate sets of independent and commuting observables: (i) $\{H_1, l_z^{(1)}, (H_z^{(1)}), H_2, l_z^{(2)}, (H_z^{(2)})\}$ and (ii) $\{H_{\text{c.m.}}, l_z^{(\text{c.m.})}, (H_z^{(\text{c.m.})}), H_{\text{rel}}^{(0)}, l_z^{(\text{rel})}, (H_z^{(\text{rel})})\}$. Simultaneously, all these observables commute with H at $V_C = 0$. Note, however, that the observables from different sets are not commuting. For example,

$$\begin{aligned} [l_z^{(1)}, l_z^{(\text{c.m.})}] &= -[l_z^{(2)}, l_z^{(\text{c.m.})}] \\ &= \frac{i\hbar}{4}(x_1 p_x^{(2)} + y_1 p_y^{(2)} - x_2 p_x^{(1)} - y_2 p_y^{(1)}), \end{aligned} \quad (8)$$

etc. It appears that the sets (i) and (ii) are two alternative CSCOs.

We recall a well known theorem: *If there are two conserved physical quantities whose operators do not commute, then the energy levels of the system are in general degenerate* (see §10 in Ref. 39). Evidently, the existence of two sets at $V_C = 0$ yields the degeneracy of the eigenenergies in our system. This degeneracy is easy to understand, taking into account two decompositions

$$H_0 \equiv H(V_C = 0) = \begin{cases} H_1 + H_2, \\ H_{\text{c.m.}} + H_{\text{rel}}^{(0)}. \end{cases} \quad (9)$$

The choice of the first or the second decomposition defines the use of the set (i) or the set (ii), respectively.

The interaction V_C breaks the symmetries of the noninteracting model related to the set (i). As a consequence, it removes the degeneracy existing in the noninteracting case. Note that the symmetries of set (ii) are, however, preserved. Below we will see that these states are generally entangled, even at $V_C \rightarrow 0$; the removal of the degeneracy by the inter-particle interaction is the key point to understanding this feature.

C. Representations

At $V_C = 0$ the integrals of motion suggest two appropriate basis sets for the orbital eigenfunctions $\psi(\mathbf{r}_1, \mathbf{r}_2)$ – the individual-particle (IP) basis with the eigenstates of the CSCO (i), and the center-of-mass–relative-motion basis with the eigenstates of the CSCO (ii). Hereafter, for the sake of convenience we name the center-of-mass–relative-motion basis/representation as the CM basis/representation.

The IP basis consists of products of eigenstates of the Hamiltonians H_1 and H_2 . In the 2D model the eigenstates of H_i and $l_z^{(i)}$ ($i = 1, 2$) are the Fock-Darwin states $\Phi_{n_i, m_i}(\mathbf{r}_i)$ [40]. In the 3D model the elements of the IP basis are $\Phi_{n_1, m_1}(\rho_1, \varphi_1) \phi_{n_{z_1}}(z_1) \Phi_{n_2, m_2}(\rho_2, \varphi_2) \phi_{n_{z_2}}(z_2)$ (see Appendix A).

In the IP representation the quantum number $M = m_1 + m_2$ is a z -projection of the total angular momentum. Since M is a good quantum number, the orbital wave function $\psi(\mathbf{r}_1, \mathbf{r}_2)$ is expanded in the IP basis with elements that are subject to the condition $m_1 + m_2 = M$. In the 2D model we have

$$\psi(\mathbf{r}_1, \mathbf{r}_2) = \sum_{n_1, n_2} \sum_{m_2=0}^M a_{n_1, n_2, m_2}^{(M)} \Phi_{n_1, M-m_2}(\mathbf{r}_1) \Phi_{n_2, m_2}(\mathbf{r}_2). \quad (10)$$

The coefficients $a_{n_1, n_2, m_2}^{(M)}$, as well as the corresponding eigenenergies, can be determined by diagonalizing the Hamiltonian matrix H in the IP (2D) basis. The interaction matrix elements $\langle n_1, m_1, n_2, m_2 | V_C | n'_1, m'_1, n'_2, m'_2 \rangle$ can be evaluated using, for example, the expressions from Sec. 2.5.1. in Ref. [41]. Of course, in numerical calculations the basis must be restricted to a finite set $(n_1, n_2 = 0, \dots, n_{\max})$ whose size is determined by the required accuracy of results. In the 3D case the expansion goes over the IP basis elements, that includes the additional summation over the indices n_{z_1} and n_{z_2} . Since the Hamiltonian H commutes with the parity operator the orbital functions have a definite parity.

For our analysis, it is convenient to use symmetric and antisymmetric counterparts of the IP basis in the orbital space. In the 2D case the corresponding basis elements are the (anti)symmetrized products of the Fock-Darwin states, which we will denote by $\{\Phi_{n_1, m_1}(\mathbf{r}_1), \Phi_{n_2, m_2}(\mathbf{r}_2)\}_{\pm}$ (see Eq. (A5) in Appendix A). Symmetric (+) and antisymmetric (−) eigenfunctions of the Hamiltonian H are expanded as

$$\psi^{(\pm)}(\mathbf{r}_1, \mathbf{r}_2) = \sum_{n_1, n_2} \sum_{m_2=0}^{[M/2]} C_{n_1, n_2, m_2}^{(M, \pm)} \times \{\Phi_{n_1, M-m_2}(\mathbf{r}_1), \Phi_{n_2, m_2}(\mathbf{r}_2)\}_{\pm}, \quad (11)$$

where $[M/2]$ is the integer part of $M/2$. This expression can be readily generalized for the 3D model. In this case we use the (anti)symmetrized products of the functions $\Phi_{n_1, m_1}(\rho_1, \varphi_1) \phi_{n_{z_1}}(z_1)$ and $\Phi_{n_2, m_2}(\rho_2, \varphi_2) \phi_{n_{z_2}}(z_2)$, and

perform the additional summation in Eq. (11) over the indices n_{z_1} and n_{z_2} .

The CM basis consists of the products of eigenstates of the Hamiltonians $H_{c.m.}$ and $H_{rel}^{(0)}$. These eigenfunctions are the Fock-Darwin states, but with the values $\mathcal{M} = 2m^*$ and $\mu = m^*/2$, respectively, instead of the effective electron mass m^* (see Appendix B).

The expansion of the orbital function $\psi(\mathbf{r}_1, \mathbf{r}_2)$ in the CM basis goes only over the relative motion quantum number(s) n (and n_z in the 3D model). This is a consequence of the fact that the CM motion is fully separable in cylindrical coordinates, and the quantum numbers $n_{c.m.}$, $m_{c.m.}$ (and $n_z^{c.m.}$), and $m = M - m_{c.m.}$, are good quantum numbers. Thus, in this representation the eigenfunctions of the Hamiltonian H are factorized as

$$\psi(\mathbf{r}_1, \mathbf{r}_2) = \psi_{c.m.}(\mathbf{R}) \psi_{rel}(\mathbf{r}_{12}). \quad (12)$$

Here $\psi_{c.m.} = \Phi_{n_{c.m.}, m_{c.m.}}^{(c.m.)}(\rho_{c.m.}, \varphi_{c.m.}) \phi_{n_z^{c.m.}}^{(c.m.)}(Z)$ are the eigenfunctions of the Hamiltonian $H_{c.m.}$, and

$$\psi_{rel} = \sum_{n, n_z} b_{n, n_z}^{(m)} \Phi_{n, m}^{(rel)}(\rho_{12}, \varphi_{12}) \phi_{n_z}^{(rel)}(z_{12}) \quad (13)$$

are the eigenfunctions of the Hamiltonian H_{rel} . In the 2D model the ϕ -functions and the summation over n_z is removed. In contrast to the IP basis, the CM basis functions have a definite exchange symmetry by construction (see Appendix B).

It seems likely that the CM representation is more convenient for calculations. However, the physical essence of quantum electron correlations is more transparent if the eigenfunctions are expanded in the IP basis.

D. Entanglement measures

The entanglement of a pure state of a bipartite quantum system can be quantified uniquely by the entropy of one of its subsystems. Namely, if the global pure state Ψ is entangled, i.e., it cannot be factorized into individual pure states of the subsystems, each of the subsystems (1 and 2) is in a mixed state. The degree of mixing can be determined by means of the von Neumann entropy $-\text{Tr}(\rho_1 \ln \rho_1) = -\text{Tr}(\rho_2 \ln \rho_2)$. Here $\rho_1 = \text{Tr}_2 |\Psi\rangle\langle\Psi|$ and $\rho_2 = \text{Tr}_1 |\Psi\rangle\langle\Psi|$ are the reduced density matrices, describing the mixed states of the subsystems 1 and 2, respectively. Alternatively, one can calculate the linear entropy $\mathcal{E} = 1 - \text{Tr} \rho_1^2 = 1 - \text{Tr} \rho_2^2$ that can be obtained from the von Neumann entropy by expanding the logarithm of the reduced density matrix and retaining the leading term. Both entropies meet the necessary requirements for an entanglement measure. The linear entropy is, however, more convenient to compute, and we will use this measure.

For the systems consisting of two identical fermions (electrons) the measure must be modified in order to exclude the contribution related to the antisymmetric character of fermionic states. The correlations due to the

Pauli principle do not contribute to the state's entanglement. For instance, a two-fermion state of a Slater rank 1 (i.e., a state represented by one Slater determinant) must be regarded as non-entangled, and its measure has to be zero. In order to satisfy this requirement, the entanglement measure based on the linear entropy in the case of two identical fermions has the form (see, for example, [14, 15, 23])

$$\mathcal{E} = 1 - 2 \text{Tr} \rho_r^2. \quad (14)$$

Here ρ_r is the reduced single-particle density matrix obtained by tracing the two-particle density matrix $\rho = |\Psi\rangle\langle\Psi|$ (describing the pure state Ψ) over one of the two particles. As a result, the measure (14) transforms to the following form for a factorized wave function (7)

$$\mathcal{E} = 1 - 2 \text{Tr}[\rho_r^{(\text{orb})2}] \text{Tr}[\rho_r^{(\text{spin})2}], \quad (15)$$

where $\rho_r^{(\text{orb})}$ and $\rho_r^{(\text{spin})}$ are the reduced single-particle density matrices in the orbital and spin spaces, respectively. In principle, the trace of $\rho_r^{(\text{orb})2}$ has to be calculated in some single-particle basis. It is convenient, however, to calculate this trace by means of the formula

$$\text{Tr}[\rho_r^{(\text{orb})2}] = \int d\mathbf{r}_1 d\mathbf{r}_1' d\mathbf{r}_2 d\mathbf{r}_2' \psi(\mathbf{r}_1, \mathbf{r}_2) \psi^*(\mathbf{r}_1', \mathbf{r}_2) \psi^*(\mathbf{r}_1, \mathbf{r}_2') \psi(\mathbf{r}_1', \mathbf{r}_2'). \quad (16)$$

The trace of $\rho_r^{(\text{spin})2}$ in the two-electron spin states with a definite symmetry χ_{S, M_S} has values: 1/2 if $M_S = 0$ (antiparallel spins of two electrons), and 1 if $M_S = \pm 1$ (parallel spins), i.e.,

$$\text{Tr}[\rho_r^{(\text{spin})2}] = \frac{1}{2}(1 + |M_S|). \quad (17)$$

III. THE LOWEST STATES – INDIVIDUAL PARTICLE DESCRIPTION

In this section, using the individual particle picture, we consider the lowest states of two-electron QDs in the magnetic field, that are characterized by different values of the quantum number M . These states represent the ground state of the system in different intervals of the magnetic field strength (see singlet-triplet transitions in Sec. VI). We study here the behaviour of these states in the limit of $V_C \rightarrow 0$.

A. The lowest energy levels and states

At $V_C = 0$, by ignoring temporarily the spin term H_S , the two-electron energy levels are defined by the sum of single-electron energies $E_{n_1, m_1, n_{z1}} + E_{n_2, m_2, n_{z2}}$ (see Eqs. (A2), (A4)). The related (unsymmetrized) eigenstates are the products $\Phi_{n_1, m_1}(\rho_1, \varphi_1) \phi_{n_{z1}}(z_1) \Phi_{n_2, m_2}(\rho_2, \varphi_2) \phi_{n_{z2}}(z_2)$ (i.e. the

IP basis, see Appendix A). The lowest levels are characterized by $n_1 = n_2 = n_{z1} = n_{z2} = 0$ and $m_1, m_2 \geq 0$, and are defined as

$$\begin{aligned} E_M^{(0)} &= E_{0, m_1, 0} + E_{0, m_2, 0} \\ &= \hbar\Omega(M+2) - \hbar\omega_L M + \hbar\omega_z, \end{aligned} \quad (18)$$

where $M = m_1 + m_2$ is the quantum number of the z -projection of the total angular momentum. The levels (18) are $M+1$ times degenerate (orbital degeneracy). Thus, all linear combinations of the IP basis states with $n_1 = n_2 = n_{z1} = n_{z2} = 0$ and $m_1 + m_2 = M$, or their (anti)symmetrized counterparts, are different eigenstates of the same level $E_M^{(0)}$. Here, since all two-electron states must have a definite exchange symmetry, it is more convenient to use linear combinations with the (anti)symmetrized basis functions.

For noninteracting electrons the Zeeman splitting yields three different levels: $E_M^{(0)} + \Delta E_{M_S}$, where $\Delta E_{M_S} = g^* \mu_B B M_S$ (see Fig. 1(a)). Obviously, for $g^* < 0$ ($g^* = -0.44$ for GaAs) the lowest triplet level corresponds to $M_S = 1$, and we will further focus on the states with $M_S = S$.

Evidently, at $V_C \neq 0$, the orbital eigenfunctions are decomposed in the IP basis in the form (10), or in the form (11), where the relation $m_1 + m_2 = M$ must be fulfilled for different values of n_1, n_2, n_{z1}, n_{z2} . The corresponding energy levels are obtained by diagonalizing the Hamiltonian H in the chosen basis. One would expect, that the lowest levels, characterized by different values of M (E_M), should converge to the levels $E_M^{(0)}$ given by Eq. (18) in the limit $V_C \rightarrow 0$. The lowest levels (including the Zeeman splitting) for $M = 0, 1, 2$ as functions of the magnetic field for a typical axially symmetric two-electron QD are shown in Fig. 1(b).

B. The limit of noninteracting electrons

As discussed above, at the limit $V_C \rightarrow 0$ it is natural to expect that the lowest levels E_M converge to the levels $E_M^{(0)}$. The same must be true for the corresponding eigenstates. This means that the expansion (11) and its 3D counterpart are reduced to the sum of contributions of the basis elements with $n_1 = n_2 = n_{z1} = n_{z2} = 0$ and different values of $m_2 = M - m_1$ only. In this case the z -component of the wave function is simply the product $\phi_0(z_1)\phi_0(z_2)$ that is decoupled from the lateral degrees of freedom. Consequently, quantum correlations appear strictly due to coupling of functions (A5) with $n_1 = n_2 = 0$. Hereafter (in this Section), for the sake of simplicity, we will drop the z -component of the wave function and, without loss of generality, consider the 2D description.

As a result, the expansion (11) is reduced to the sum

$$\psi^{(M, \pm)}(\mathbf{r}_1, \mathbf{r}_2) = \sum_{k=1}^{d_{\pm}} c_k^{(M, \pm)} u_k^{(M, \pm)}(\mathbf{r}_1, \mathbf{r}_2), \quad (19)$$

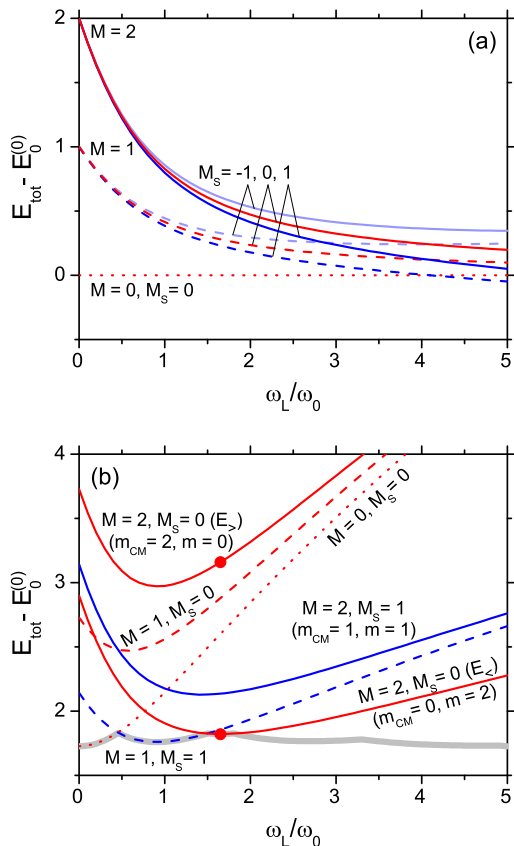


FIG. 1: (Color online) Lowest energy levels (in $\hbar\omega_0$ units) of an axially symmetric two-electron QD with $\omega_z \gg \omega_0$ for: (a) noninteracting electrons ($\lambda = 0$) and (b) $\lambda = 2$ (in $\hbar\omega_0\ell_0$ units). In order to get a better resolution the energy are defined with respect to the $E_0^{(0)}$ level. The Zeeman splitting is taken into account: the effective Landé factor $g^* = -0.44$. Closed circles mark the $M = 2$ and $M_S = 0$ levels at the field strength $\omega_L/\omega_0 = 1.65$. At this value the lower level ($E_<$) corresponds to the ground state energy (thick gray line).

where the index $k = m_2 + 1$ counts the basis states (A5) of a given symmetry (\pm) with $n_1 = n_2 = 0$ and a given M , i.e.,

$$u_k^{(M,\pm)}(\mathbf{r}_1, \mathbf{r}_2) = \{\Phi_{0,M-k+1}(\mathbf{r}_1), \Phi_{0,k-1}(\mathbf{r}_2)\}_{\pm}. \quad (20)$$

Here

$$c_k^{(M,\pm)} = \lim_{V_C \rightarrow 0} C_{0,0,m_2}^{(M,\pm)} \quad (21)$$

are the limiting values of the non-vanishing coefficients. Occasionally, the notation M in the superscript (M, \pm) will be dropped, when we deal with a fixed value of the quantum number M . The explicit expressions for basis states (20) for $M = 0, 1, 2, 3$ are given in Table I. The sum (19) has $d_{\pm} = [M/2] + 1$ terms, except the antisymmetric case with an even M , when $d_- = [M/2]$ [because $\{\Phi_{0,m_1}(\mathbf{r}_1), \Phi_{0,m_2}(\mathbf{r}_2)\}_- = 0$ when $m_1 = m_2$]. In general, one can write $d_{\pm} = [M/2] + 1/2 + (\pm 1)^{M+1}/2$. These numbers can be treated as the partial degeneracies of

TABLE I: Basis states $u_k^{(M,\pm)}$ [Eq. (20)] for $M = 0, 1, 2, 3$.

M	basis function
0	$u_1^{(0,+)}(\mathbf{r}_1, \mathbf{r}_2) = \Phi_{0,0}(\mathbf{r}_1)\Phi_{0,0}(\mathbf{r}_2)$
1	$u_1^{(1,\pm)}(\mathbf{r}_1, \mathbf{r}_2) = \frac{1}{\sqrt{2}}[\Phi_{0,1}(\mathbf{r}_1)\Phi_{0,0}(\mathbf{r}_2) \pm \Phi_{0,0}(\mathbf{r}_1)\Phi_{0,1}(\mathbf{r}_2)]$
2	$u_1^{(2,\pm)}(\mathbf{r}_1, \mathbf{r}_2) = \frac{1}{\sqrt{2}}[\Phi_{0,2}(\mathbf{r}_1)\Phi_{0,0}(\mathbf{r}_2) \pm \Phi_{0,0}(\mathbf{r}_1)\Phi_{0,2}(\mathbf{r}_2)]$ $u_2^{(2,+)}(\mathbf{r}_1, \mathbf{r}_2) = \Phi_{0,1}(\mathbf{r}_1)\Phi_{0,1}(\mathbf{r}_2)$
3	$u_1^{(3,\pm)}(\mathbf{r}_1, \mathbf{r}_2) = \frac{1}{\sqrt{2}}[\Phi_{0,3}(\mathbf{r}_1)\Phi_{0,0}(\mathbf{r}_2) \pm \Phi_{0,0}(\mathbf{r}_1)\Phi_{0,3}(\mathbf{r}_2)]$ $u_2^{(3,\pm)}(\mathbf{r}_1, \mathbf{r}_2) = \frac{1}{\sqrt{2}}[\Phi_{0,2}(\mathbf{r}_1)\Phi_{0,1}(\mathbf{r}_2) \pm \Phi_{0,1}(\mathbf{r}_1)\Phi_{0,2}(\mathbf{r}_2)]$

the level $E_M^{(0)}$, that take into account only the states of a given exchange symmetry ($d_+ + d_- = M + 1$). The coefficients in the expansion (19) can be determined exactly by diagonalizing the Hamiltonian H (in the same limit) in the finite set ($k = 1, \dots, d_{\pm}$) of states (20). In fact, in the limit $V_C \rightarrow 0$ the full diagonalization procedure is reduced to the first order degenerate perturbation approach. Below we study the lowest states with $M = 0, 1, 2, 3$ in the limit $V_C \rightarrow 0$.

1. The lowest $M = 0$ state

At $M = 0$ the magnetic quantum numbers of individual electrons are $m_1 = m_2 = 0$. The orbital degeneracy at $V_C = 0$ is 1 ($d_+ = 1$ and $d_- = 0$), and the only basis state in the expansion (19) is $u_1^{(+)}$ (see Table I). Therefore, the lowest $M = 0$ eigenstate of H in the limit $V_C \rightarrow 0$ is

$$\psi^{(+)}(\mathbf{r}_1, \mathbf{r}_2) = u_1^{(+)}(\mathbf{r}_1, \mathbf{r}_2) \equiv \Phi_{0,0}(\mathbf{r}_1)\Phi_{0,0}(\mathbf{r}_2). \quad (22)$$

Due to the Pauli principle the related spin state is a singlet ($S = M_S = 0$). Since it is antisymmetric, the total wave function has the form of the Slater determinant, and the entanglement of the lowest state with $M = 0$ must be zero.

2. The lowest $M = 1$ states

At $M = 1$, one has: ($m_1 = 1, m_2 = 0$) or ($m_1 = 0, m_2 = 1$). Thus, the orbital degeneracy is 2 ($d_+ = d_- = 1$). We have two basis states, $u_1^{(+)}$ and $u_1^{(-)}$ (see Table I), that may appear in the expansion (19). However, due to different symmetries these states cannot create a superposition. As a result, the lowest $M = 1$ eigenstate is one of them, depending on the initially chosen symmetry, i.e.,

$$\begin{aligned} \psi^{(\pm)}(\mathbf{r}_1, \mathbf{r}_2) &= u_1^{(\pm)}(\mathbf{r}_1, \mathbf{r}_2) \\ &\equiv \frac{1}{\sqrt{2}}[\Phi_{0,1}(\mathbf{r}_1)\Phi_{0,0}(\mathbf{r}_2) \pm \Phi_{0,0}(\mathbf{r}_1)\Phi_{0,1}(\mathbf{r}_2)]. \end{aligned} \quad (23)$$

For $u_1^{(+)}$ the related spin state is the singlet, whereas for $u_1^{(-)}$ we have the triplet state. Here we choose the triplet state ($S = M_S = 1$) which is lower. Since this spin state is the product of individual electron spin states with $m_s = +1/2$, the total wave function of the lowest $M = 1$ state is a Slater determinant and its entanglement is again zero.

3. The lowest $M = 2$ states

At $M = 2$ one has: $(m_1 = 2, m_2 = 0)$, or $(m_1 = 1, m_2 = 1)$, or $(m_1 = 0, m_2 = 2)$. The orbital degeneracy is 3 ($d_+ = 2, d_- = 1$). As a result, we have three basis states: two symmetric ($u_1^{(+)}, u_2^{(+)}$), and one anti-symmetric ($u_1^{(-)}$) (see Table I). The related spin states are: singlet, singlet and triplet, respectively. At $V_C = 0$ the triplet state (due to the Zeeman splitting) produces a lower energy (see Fig. 1(a)). However, at $V_C \neq 0$ and typical values of the effective Landé factor the lowest energy level with $M = 2$ corresponds to the singlet state (see Fig. 1(b)). Due to this fact, at $M = 2$, we will focus on the orbital symmetric states and study their behaviour in the limit $V_C \rightarrow 0$.

At $V_C = 0$ the lowest ($M = 2, S = 0$) level is doubly degenerate ($d_+ = 2$). As a result, the orbital wave function may be any superposition of the states $u_1^{(+)}$ and $u_2^{(+)}$, i.e.,

$$\psi^{(+)}(\mathbf{r}_1, \mathbf{r}_2) = c_1 u_1^{(+)}(\mathbf{r}_1, \mathbf{r}_2) + c_2 u_2^{(+)}(\mathbf{r}_1, \mathbf{r}_2). \quad (24)$$

Here the coefficients c_1 and c_2 are arbitrary complex numbers that are subject to the condition $|c_1|^2 + |c_2|^2 = 1$ (green circular line in Fig. 2(a)). In this case it is always possible to choose a set of eigenstates exhibiting zero entanglement, e.g., $\psi_1^{(+)} = u_1^{(+)}$ and $\psi_2^{(+)} = u_2^{(+)}$ (blue open circles) in Fig. 2(a)).

The nonzero interaction between the electrons couples not only the functions $u_1^{(+)}$ and $u_2^{(+)}$, but also the symmetric functions (A5) with $m_1 + m_2 = M$ and $n_1, n_2 > 0$. They will contribute to a given state with specific values of the expansion coefficients in (11). For the lowest states, however, the terms with $n_1 = n_2 = 0$ are dominant, even at $V_C \neq 0$. As a result, the corresponding coefficients (here $C_{0,0,m_2}^{(2,+)}$, with $m_2 = 0, 1$) practically determine the states (red closed circles in Fig. 2(b)).

By treating $V_C = \lambda/r_{12}$ as a small perturbation, the coefficients c_1 and c_2 can be determined exactly in the limit $\lambda \rightarrow 0$, using the first order degenerate perturbation theory. One obtains the following set of linear equations

$$\begin{aligned} (\lambda V_{11} - \Delta E)c_1 + \lambda V_{12}c_2 &= 0, \\ \lambda V_{21}c_1 + (\lambda V_{22} - \Delta E)c_2 &= 0, \end{aligned} \quad (25)$$

where $V_{ij} = \langle u_i^{(+)} | r_{12}^{-1} | u_j^{(+)} \rangle$ and $\Delta E = E - E_2^{(0)}$. The correction to the energy ΔE follows from the requirement

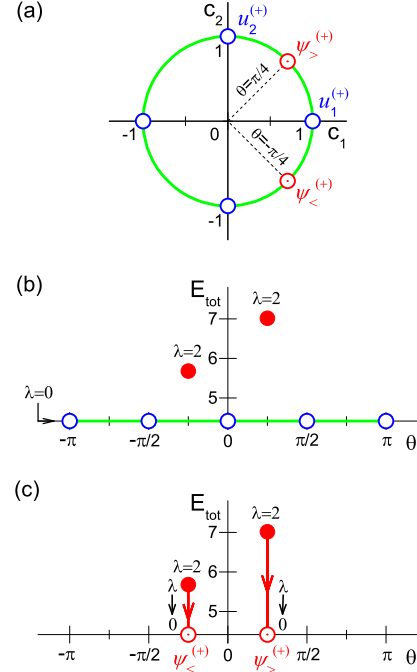


FIG. 2: (Color online) (a) Full range of (real) values of the coefficients c_1 and c_2 in the superposition (24) that represents the lowest symmetric orbital states $\psi^{(+)}$ with $M = 2$ at $\lambda = 0$ (green circular line) and in the limit $\lambda \rightarrow 0$ (red \odot symbols). The values, marked by (blue) open circles, correspond to the uncorrelated basis states $\pm u_1^{(+)}$ and $\pm u_2^{(+)}$. (b) Lowest $\psi^{(+)}$ states with $M = 2$ and the related eigenenergies (in $\hbar\omega_0$ units) are shown in the θ - E_{tot} diagram, where $\theta = \arctan(c_2/c_1)$, for $\lambda = 0$ (green line) and $\lambda = 2$ (red closed circles) (in $\hbar\omega_0 \ell_0$ units). The full θ -domain ($\theta \in (-\pi, \pi)$), that corresponds to $\lambda = 0$ (degenerate level $E_2^{(0)}$), is reduced to two discrete values ($\theta \approx \pm\pi/4$) as soon as the interaction is switched on. The eigenenergies are calculated for $\omega_L/\omega_0 = 1.65$ [at $\lambda = 2$ the state at $\theta \approx -\pi/4$ is the ground state; see Fig. 1(b)]. (c) The θ - E_{tot} diagram (the energy is in $\hbar\omega_0$ units) showing the transition of the lowest (orbital symmetric) states at $\lambda = 2$ to the states $\psi_{\pm}^{(+)}$ (see Eq. (30)), obtained by reducing gradually the interaction. The states remain entangled at any $\lambda \neq 0$ ($\theta \approx \pm\pi/4$), even in the limit $\lambda \rightarrow 0$ (then $\theta = \pm\pi/4$).

that the determinant of this system must be equal to zero (a secular equation). As a result, one has

$$\Delta E_{\geq} = \frac{\lambda}{2} \left[V_{11} + V_{22} \pm \sqrt{(V_{11} - V_{22})^2 + 4V_{12}V_{21}} \right]. \quad (26)$$

Using one of Eqs.(25) and the condition $|c_1|^2 + |c_2|^2 = 1$, we obtain

$$c_1 = \frac{V_{12}}{\sqrt{(V_{11} - \Delta E/\lambda)^2 + V_{12}^2}}, \quad (27)$$

$$c_2 = -\frac{V_{11} - \Delta E/\lambda}{\sqrt{(V_{11} - \Delta E/\lambda)^2 + V_{12}^2}}. \quad (28)$$

The interaction matrix elements V_{ij} can be numerically evaluated exactly (by means of the analytical expression for the matrix elements $\langle m_1, m_2 | r_{12}^{-1} | m'_1, m'_2 \rangle$ given in Ref. 41). For $M = 2$ one has $V_{11} = V_{22} = 0.86165$, $V_{12} = V_{21} = 0.39166$. As a result, we obtain

$$\Delta E_{\geq} = \lambda(V_{11} \pm V_{12}) \quad (29)$$

and $c_1 = \pm c_2 = 1/\sqrt{2}$. Thus, the related states are

$$\begin{aligned} \psi_{\geq}^{(+)}(\mathbf{r}_1, \mathbf{r}_2) &= \frac{1}{\sqrt{2}}[u_1^{(+)}(\mathbf{r}_1, \mathbf{r}_2) \pm u_2^{(+)}(\mathbf{r}_1, \mathbf{r}_2)] \\ &\equiv \frac{1}{2} \Phi_{0,2}(\mathbf{r}_1) \Phi_{0,0}(\mathbf{r}_2) \\ &\pm \frac{1}{\sqrt{2}} \Phi_{0,1}(\mathbf{r}_1) \Phi_{0,1}(\mathbf{r}_2) \\ &+ \frac{1}{2} \Phi_{0,0}(\mathbf{r}_1) \Phi_{0,2}(\mathbf{r}_2). \end{aligned} \quad (30)$$

In the diagrams in Fig. 2 these states are marked by the symbol \odot . Note that the both solutions correspond to the energy $E_2^{(0)}$ ($\Delta E_{\geq} \rightarrow 0$ in the limit $\lambda \rightarrow 0$). However, if we start from the lowest ($M = 2, S = 0$) state of interacting electrons, the system approaches the state $\psi_{<}^{(+)} = (u_1^{(+)} - u_2^{(+)})/\sqrt{2}$ in the limit $\lambda \rightarrow 0$.

Thus, in the limit $V_C \rightarrow 0$ the lowest ($M = 2, S = 0$) states will converge to the states (24) with the specific values of the coefficients c_1 and c_2 (the states (30)). In contrast, at $V_C = 0$ these coefficients could be chosen to be arbitrary. The interaction removes the degeneracy present in the noninteracting case, and leads the system (even in the limit $V_C \rightarrow 0$) to an uniquely determined entangled state. Indeed, it cannot be reduced to a single Slater determinant. This is essentially the same mechanism, discussed in a qualitative manner in Ref. 42.

4. The lowest $M = 3$ states

At $M = 3$ one has: ($m_1 = 3, m_2 = 0$), or ($m_1 = 2, m_2 = 1$), or ($m_1 = 1, m_2 = 2$), or ($m_1 = 0, m_2 = 3$). The orbital degeneracy is 4 ($d_+ = d_- = 2$). As a result, we have four basis states, two symmetric and two antisymmetric: $u_1^{(\pm)}, u_2^{(\pm)}$ (see Table I). The orbital functions $u_i^{(+)}$ and $u_i^{(-)}$ correspond to the singlet and triplet spin states, respectively. For odd M the lowest energy level, for both noninteracting and interacting electrons, corresponds to the triplet state with $M_S = 1$ (not shown in Fig. 1). Therefore, we consider the antisymmetric orbital states.

For noninteracting electrons the lowest level ($M = 3, S = M_S = 1$) is doubly degenerate ($d_- = 2$). Therefore, the orbital wave function may be any superposition of the states $u_1^{(-)}$ and $u_2^{(-)}$ with arbitrary coefficients c_1 and c_2 that are subject to the condition $|c_1|^2 + |c_2|^2 = 1$. Again, due to the degeneracy, it is possible to choose the set of eigenstates, exhibiting a zero entanglement. For interacting electrons, however, this state will converge to

the state $\psi^{(-)} = c_1 u_1^{(-)} + c_2 u_2^{(-)}$ with specific values of the coefficients c_1 and c_2 in the limit $V_C \rightarrow 0$.

Indeed, applying the first order degenerate perturbation theory, by means of Eqs.(26), (27), (28), and the corresponding values of the interaction matrix elements for $M = 3$ [$V_{11} = 0.56791, V_{22} = 0.45041, V_{12} = V_{21} = \sqrt{3}(V_{11} - V_{22})/2 = 0.10176$], we obtain

$$\Delta E_{\geq} = \frac{\lambda}{2}[(V_{11} + V_{22}) \pm 2(V_{11} - V_{22})]. \quad (31)$$

For $\Delta E_{<}$ we have $c_1 = 1/2, c_2 = -\sqrt{3}/2$; and for $\Delta E_{>}$ we have $c_1 = \sqrt{3}/2, c_2 = 1/2$. Thus, the related states are

$$\begin{aligned} \psi_{<}^{(-)}(\mathbf{r}_1, \mathbf{r}_2) &= \frac{1}{2}[u_1^{(-)}(\mathbf{r}_1, \mathbf{r}_2) - \sqrt{3}u_2^{(-)}(\mathbf{r}_1, \mathbf{r}_2)] \\ &\equiv \frac{1}{2\sqrt{2}}[\Phi_{0,3}(\mathbf{r}_1) \Phi_{0,0}(\mathbf{r}_2) \\ &\quad - \sqrt{3} \Phi_{0,2}(\mathbf{r}_1) \Phi_{0,1}(\mathbf{r}_2) \\ &\quad + \sqrt{3} \Phi_{0,1}(\mathbf{r}_1) \Phi_{0,2}(\mathbf{r}_2) \\ &\quad - \Phi_{0,0}(\mathbf{r}_1) \Phi_{0,3}(\mathbf{r}_2)], \end{aligned} \quad (32)$$

$$\begin{aligned} \psi_{>}^{(-)}(\mathbf{r}_1, \mathbf{r}_2) &= \frac{1}{2}[\sqrt{3}u_1^{(-)}(\mathbf{r}_1, \mathbf{r}_2) + u_2^{(-)}(\mathbf{r}_1, \mathbf{r}_2)] \\ &\equiv \frac{1}{2\sqrt{2}}[\sqrt{3} \Phi_{0,3}(\mathbf{r}_1) \Phi_{0,0}(\mathbf{r}_2) \\ &\quad + \Phi_{0,2}(\mathbf{r}_1) \Phi_{0,1}(\mathbf{r}_2) \\ &\quad - \Phi_{0,1}(\mathbf{r}_1) \Phi_{0,2}(\mathbf{r}_2) \\ &\quad - \sqrt{3} \Phi_{0,0}(\mathbf{r}_1) \Phi_{0,3}(\mathbf{r}_2)]. \end{aligned} \quad (33)$$

Note that the both solutions correspond to the energy $E_3^{(0)}$. However, if we start from the lowest ($M = 3, S = M_S = 1$) state of interacting electrons, the system in the limit $\lambda \rightarrow 0$ approaches the state $\psi_{<}^{(-)} = (u_1^{(-)} - \sqrt{3}u_2^{(-)})/2$. As in the previous case, the lowest $M = 3$ state is entangled because it cannot be reduced to a single Slater determinant.

C. Entanglement of the lowest states in the limit $V_C \rightarrow 0$

In the general case (within the 2D model) the lowest eigenstates with $M = 0, 1, 2, 3$ of the Hamiltonian H in the IP basis can be written in the form

$$\psi^{(\pm)}(\mathbf{r}_1, \mathbf{r}_2) = \sum_{m_2=0}^M a_{m_2}^{(\pm)} \Phi_{0, M-m_2}(\mathbf{r}_1) \Phi_{0, m_2}(\mathbf{r}_2), \quad (34)$$

where the coefficients $a_{m_2}^{(\pm)}$ can be expressed in terms of the coefficients $c_k^{(\pm)}$ in the expansion (19). The reduced

density matrix of the state (10), calculated in the single-particle Fock-Darwin basis, will be a sum consisting of $M + 1$ terms. For example,

$$\rho_1^{(\text{orb})} = \text{Tr}_2 |\psi\rangle\langle\psi| = \sum_{m_2=0}^M {}_2\langle m_2|\psi\rangle\langle\psi|m_2\rangle_2, \quad (35)$$

where ${}_2\langle m_2|\psi\rangle$ denotes the (partial) scalar product between the Fock-Darwin state $\Phi_{0,m_2}(\mathbf{r}_2)$ and the orbital state $\psi(\mathbf{r}_1, \mathbf{r}_2)$. For the state (34) one has ${}_2\langle m_2|\psi^{(\pm)}\rangle = a_{m_2}^{(\pm)}|M - m_2\rangle_1 = a_{m_1}^{(\pm)}|m_1\rangle_1$, where $m_1 = M - m_2$. Here the Dirac ket $|m_1\rangle_1$ corresponds to the Fock-Darwin state $\Phi_{0,m_1}(\mathbf{r}_1)$. Thus, we have

$$\begin{aligned} \rho_1^{(\text{orb})} &= \sum_{m_2=0}^M |a_{m_2}^{(\pm)}|^2 |M - m_2\rangle_1 \langle M - m_2| \\ &= \sum_{m_1=0}^M |a_{M-m_1}^{(\pm)}|^2 |m_1\rangle_1 \langle m_1|. \end{aligned} \quad (36)$$

In fact, the reduced density matrix is diagonal in the Fock-Darwin basis. One obtains readily its square

$$\rho_1^{(\text{orb})2} = \sum_{m_1=0}^M |a_{M-m_1}^{(\pm)}|^4 |m_1\rangle_1 \langle m_1| \quad (37)$$

and the trace

$$\text{Tr}[\rho_r^{(\text{orb})2}] = \sum_{m_1=0}^M |a_{M-m_1}^{(\pm)}|^4 = \sum_{m_2=0}^M |a_{m_2}^{(\pm)}|^4. \quad (38)$$

Finally, the entanglement measure \mathcal{E} can be obtained by means of Eqs. (15), (17), (38).

The results for $M = 0, 1, 2, 3$ are shown in Table II. One can see that, in agreement with the analysis from the previous subsection, in the case of vanishing electron-electron interaction ($V_C \rightarrow 0$) the lowest states with $M = 0, 1$ are not entangled ($\mathcal{E} = 0$), while those with $M = 2, 3$ are entangled ($\mathcal{E} > 0$).

We would like to point out that the coefficients $a_{m_2}^{(\pm)}$ determine solely the trace (38), i.e., the entanglement measure \mathcal{E} . It appears that the decomposition (34) in terms of the Fock-Darwin states is similar to the Schmidt decomposition for a helium atom (see, e.g., Refs. 20, 21).

IV. THE LOWEST STATES IN THE CM REPRESENTATION

A. Classification of the lowest states

In the CM basis the determination of the wave function $\psi(\mathbf{r}_1, \mathbf{r}_2)$ is reduced to the calculation of $\psi_{\text{rel}}(\mathbf{r}_{12})$ in the form of the expansion (13). In this representation each state is characterized by the CM quantum numbers: $n_{c.m.}$, $m_{c.m.}$ and (in the 3D model) $n_z^{c.m.}$, as well as by

TABLE II: Entanglement measure based on the linear entropy \mathcal{E} and the corresponding orbital and spin factors (traces) for the lowest states with $M = 0, 1, 2, 3$ in the limit of noninteracting electrons.

M	$S(M_S)$	$\text{Tr}[\rho_r^{(\text{orb})2}]$	$\text{Tr}[\rho_r^{(\text{spin})2}]$	\mathcal{E}
0	0	1	1/2	0
1	1	1/2	1	0
2	0	3/8	1/2	5/8
3	1	5/16	1	3/8

the magnetic quantum number for the relative motion m . The total quantum numbers M , S and M_S (and the related exchange symmetry and parity) are good quantum numbers as well as in the IP representation.

The quantum numbers $m_{c.m.}$, m and M , however, are not independent ($M = m_{c.m.} + m$), and for labeling the states it is sufficient to use two of them. Moreover, in the lowest states also the values of the spin quantum numbers S and M_S depend on m . Namely, for these states the parity of the wave function ψ_{rel} is $(-1)^m$. This rule holds even in the 3D model, since the leading term in the expansion (13) is $\Phi_{0,m}^{(\text{rel})} \phi_0^{(\text{rel})}$ and, thus, all n_z must be even. As a result, due to the Pauli principle, the total spin is determined by the expression $S = \frac{1}{2}[1 - (-1)^m]$.

The quantum number M_S , on the other hand, is not directly determined by the parity. For even m we have $S = 0$ and, thus, $M_S = 0$. If m is odd, we have $S = 1$, and M_S can be $-1, 0$, or 1 . At nonzero magnetic field the Zeeman splitting ($g^* < 0$) will lower the energy of the $M_S = 1$ component of the triplet states, while leaving the singlet states unchanged. Therefore, the lowest states are characterized by

$$M_S = S = \frac{1 - (-1)^m}{2}. \quad (39)$$

Consequently, the lowest states (by considering various values of M) can be uniquely labeled by the pair of quantum numbers (M, m) or by the pair $(m_{c.m.}, m)$ (here $n_{c.m.} = n_z^{c.m.} = 0$).

At $V_C = 0$ the quantum numbers $m_{c.m.}$ and m play symmetric roles [analogously to the quantum numbers m_1 and m_2 in Eq. (18)]. As a result, one obtains that the energy levels $E_M^{(0)}$ (here constructed as $E_{c.m.} + E_{\text{rel}}^{(0)}$) are $M + 1$ times degenerate. However, at $V_C \neq 0$ the spectra of the Hamiltonians $H_{c.m.}$ and H_{rel} are different, and the degeneracy is removed. In this case the lowest states correspond to $m = M$ (i.e. $m_{c.m.} = 0$), as one can see from the example shown in Fig. 1(b). This feature can be explained by the fact that the energy contribution due to the Coulomb interaction $\Delta E^{(c)}$ in E_{rel} ($E_{\text{rel}} = E_{\text{rel}}^{(0)} + \Delta E^{(c)}$) decreases if m increases. In other words, a rotational motion of electrons attenuates the interaction. Thus, for a given M the total energy $E_{M,m} = E_M^{(0)} +$

$\Delta E_m^{(c)}$ is minimal at $m = M$.

B. Calculation of the measure \mathcal{E}

In a general case it is convenient to calculate the entanglement measure (15) by evaluating the integral (16) and the expression (17). Combining the later with Eq. (39), we obtain for the lowest states the expression for the spin contribution

$$\text{Tr}[\rho_r^{(\text{spin})2}] = \frac{3 - (-1)^m}{4}. \quad (40)$$

The orbital contribution (16) of the lowest CM eigenstate ($n_{c.m.} = m_{c.m.} = n_z^{c.m.} = 0$), applying the factorization (12) and the expansion (13), takes the form

$$\begin{aligned} \text{Tr}[\rho_r^{(\text{orb})2}] = & \sum_{n_1=0}^{n_{\max}} \sum_{n_2=0}^{n_{\max}} \sum_{n_3=0}^{n_{\max}} \sum_{n_4=0}^{n_{\max}} \sum_{n_{z_1}=0}^{n_z^{\max}} \sum_{n_{z_2}=0}^{n_z^{\max}} \sum_{n_{z_3}=0}^{n_z^{\max}} \sum_{n_{z_4}=0}^{n_z^{\max}} \\ & b_{n_1, n_{z_1}}^{(m)} b_{n_2, n_{z_2}}^{(m)} b_{n_3, n_{z_3}}^{(m)} b_{n_4, n_{z_4}}^{(m)} \times \\ & I(n_1, n_2, n_3, n_4; m) \times \\ & J(n_{z_1}, n_{z_2}, n_{z_3}, n_{z_4}), \end{aligned} \quad (41)$$

where I and J are multiple integrals of the products of four functions $\Phi_{n,m}^{(c.m.)}$ and $\phi_{n_z}^{(c.m.)}$ with different values of the indices n and n_z , respectively. Their explicit forms are given in Appendix C.

In the 2D model the trace (41) is reduced to the form with four sums via n_i ($i = 1, 2, 3, 4$). Formally it follows if we put $n_z^{\max} = 0$ and drop the J integrals (because $J(0, 0, 0, 0) = 1$).

The values of I and J integrals can be determined analytically. In particular, for $n_1 = n_2 = n_3 = n_4 = 0$ one has

$$I(0, 0, 0, 0; m) = \frac{(2|m|)!}{(2^{|m|}|m|!)^2}. \quad (42)$$

Generally, the I and J integrals do not depend on the QD parameters (e.g. Ω and ω_z , see Appendix C). Thus the variation of the entanglement $\mathcal{E}(\Omega)$ is brought about by the expansion coefficients in (13) that depend on the interaction and the magnetic field strengths. Some properties of the I and J integrals are given in Appendix C.

C. The dependance of the measure \mathcal{E} on the electron-electron interaction strength

The measure \mathcal{E} as a function of λ for the lowest states is obtained by calculating the trace (41) with $n_{\max} = 4$ and $n_z^{\max} = 0$ (the 2D model) and $n_z^{\max} = 4$ (the 3D model) (see Fig. 3). This basis size is found to be sufficient for the lowest states.

In the limit $\lambda \rightarrow 0$ the measure \mathcal{E} vanishes for $m = 0$ and $m = 1$ and converges to non-zero values for $m \geq 2$,

independently of the magnetic field strength. This result is in agreement with the results of Sec. III (see Table II). With the increase of the interaction strength λ the measure \mathcal{E} increases, since the interaction introduces additional correlations. However, for the states with larger values of m this change is slow. It appears that for typical QDs ($\lambda \sim 2 \times \hbar\omega_0 l_0$) the measure \mathcal{E} for $m \geq 2$ can be approximated by its value obtained at the noninteracting case.

The entanglement of the lowest states depends on the ratio ω_z/ω_0 . This dependence is very weak for the states with large m (see Fig. 3). This means that for typical QDs the 2D model is good enough if we calculate the entanglement of the lowest states with $m \geq 2$. On the other hand, for the lowest states with $m = 0$ and $m = 1$ this model may be insufficient.

At $B = 0$ the entanglement decreases if the ratio ω_z/ω_0 decreases from ∞ (the 2D model) to 1 (the spherically symmetric 3D model); see Fig. 3(a) and Fig. 4 at $\omega_L/\omega_0 = 0$. This effect can be explained by introducing the effective charge λ_{eff} [34, 36]. As pointed out in Ref. 36, in a 3D dot the electrons can avoid each other more effectively than in the corresponding 2D one. As a result, the Coulomb interaction has a smaller effect on the 3D spectrum than on the 2D one. The ratio $\lambda_{\text{eff}}/\lambda$ as a function of Ω/ω_z for different m is shown in Fig. 2 in Ref. 34. The maximal repulsion at $\Omega/\omega_z = 0$ corresponds with $\omega_z \rightarrow \infty$ to the 2D case and decreases monotonically as Ω/ω_z increases. Thus, a reduction of the ratio ω_z/ω_0 has an effect analogous to the reduction of the electron-electron interaction.

If $B \neq 0$, the entanglement measure \mathcal{E} is not necessarily a monotonic function of the ratio ω_z/ω_0 . In contrast to the zero-magnetic-field case, for example, at $\omega_L/\omega_0 = 2.5$ [see Fig. 3(b)] the lowest states are more entangled for the ratio $\omega_z/\omega_0 = 2$ (dashed lines) in comparison with the ratio $\omega_z/\omega_0 = 5$ (dash-dotted lines). This behavior can be understood by analyzing the dependence of the entanglement of the lowest states on the magnetic field (see the next subsection). Regarding the latest example, Fig. 4 shows how the values of \mathcal{E} for $\omega_z/\omega_0 = 2$ and $= 5$ exchange the order between $\omega_L/\omega_0 = 0$ and $= 2.5$ (the case $m = 0$ is shown).

D. The dependence of the measure \mathcal{E} on the magnetic field strength

For extremely thin QDs (described with the aid of the 2D model), the entanglement of the lowest states decreases monotonically by increasing the magnetic field strength (see Fig. 4). Evidently, the effective confinement (Ω) increases with the magnetic field, and the contribution of the constant electron-electron interaction becomes weaker. Formally, if we introduce the characteristic length of the effective confinement $\ell_\Omega = \sqrt{\hbar/m^*\Omega}$, the parameter $\lambda_\Omega = \ell_\Omega/a^*$ (R_W at $B = 0$) determines the relative strength of the Coulomb interaction at a given ef-

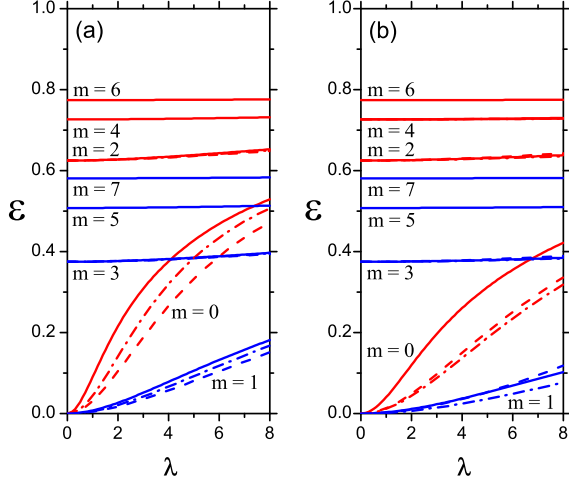


FIG. 3: (Color online) Entanglement measure \mathcal{E} of the lowest states with different m as functions of the of electron-electron interaction strength (the parameter λ in $\hbar\omega_0\ell_0$ units): for (a) $\omega_L = 0$ and (b) $\omega_L/\omega_0 = 2.5$. The dashed, dash-dotted and solid lines correspond to the (3D) QDs with $\omega_z/\omega_0 = 2$ and $\omega_z/\omega_0 = 5$ and to the 2D model of QD, respectively. The red and the blue values correspond to the symmetric and antisymmetric orbital states (i.e., even and odd $\psi_{\text{rel}}(\mathbf{r}_{12})$ functions), respectively.

fective confinement [43]. This parameter decreases with an increase of the magnetic field strength. It tends to zero at $B \rightarrow \infty$, since the Coulomb interaction becomes negligible compared to the effective confinement.

In 3D cases, however, with an increase of the magnetic field the entanglement decreases until the parameter ω_L reaches the value $\omega_L^{\text{sph}} = (\omega_z^2 - \omega_0^2)^{1/2}$. At this value the QD owns a spherical symmetry ($\Omega/\omega_z = 1$). After this value the measure starts to increase with an increase of the magnetic field (see Fig. 4). This behavior can be explained by the influence of the magnetic field on the effective strength λ_Ω . It is twofold – the magnetic field, besides the effective confinement, affects the effective charge, too. In fact, the entanglement indicates a geometrical crossover in two-electron QDs. In particular, the lateral electron density distribution transforms to the vertical one for a state with a given value of the magnetic quantum number m . A detailed analysis of this phenomenon for $m = 0$ state is presented in Refs. 32, 33.

Note that the effect of the magnetic field on the measure \mathcal{E} for states with large quantum number m is less pronounced than for the $m = 0$ state (see Fig. 6(b) for the 2D case and in Fig. 7 for 3D case).

E. The limit of noninteracting electrons

At $V_C = 0$ the lowest eigenstates of the Hamiltonian H_{rel} converge to the lowest eigenstates of the Hamilto-

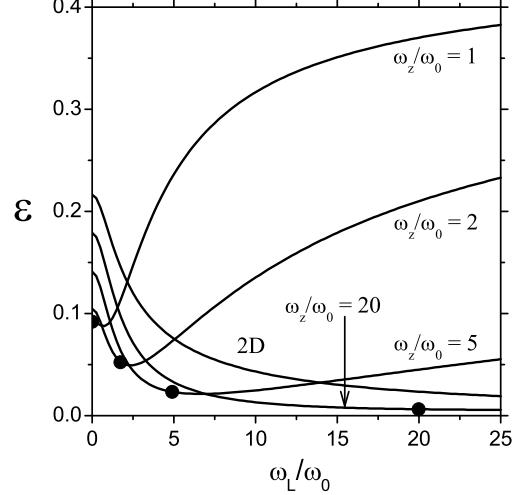


FIG. 4: Entanglement of the lowest state with $m = 0$ of axially symmetric two-electron QDs with $\lambda = 2$ (in $\hbar\omega_0\ell_0$ units) and different ratios ω_z/ω_0 as a function of the parameter ω_L/ω_0 . The closed circles denote the values of ω_L/ω_0 when the dots with the given ratios ω_z/ω_0 become spherically symmetric.

nian $H_{\text{rel}}^{(0)}$, and the orbital wave functions (12) take the form

$$\psi = \Phi_{0,0}^{(c.m.)} \phi_0^{(c.m.)} \Phi_{0,m}^{(\text{rel})} \phi_0^{(\text{rel})}. \quad (43)$$

In this limit all coefficients in the expansion (13) tend to zero, except the first one ($b_{0,0}^{(m)}$) that tends to one. As a result, Eq. (41) is reduced to a single term

$$\text{Tr}[\rho_r^{(\text{orb})2}] = I(0, 0, 0, 0; m) \quad (44)$$

(here we used $J(0, 0, 0, 0) = 1$). By means of Eqs. (15), (42), (44), (40), we obtain the result

$$\mathcal{E} = 1 - \frac{3 - (-1)^m}{2} \frac{(2m)!}{(2^m m!)^2}, \quad (45)$$

that exactly reproduces the results given in Table II (here $M = m$). The formula (45) is valid for the 2D and the 3D models of QDs.

The entanglement increases differently for even and odd values of m (see Fig. 5). This staggering is due to the spin contribution (40), whereas the orbital part is responsible for the growth of \mathcal{E} with m . Finally, since $I(0, 0, 0, 0; m) \rightarrow 0$ when $m \rightarrow \infty$, both series converge to 1, i.e.,

$$\lim_{m \rightarrow \infty} \mathcal{E} = 1. \quad (46)$$

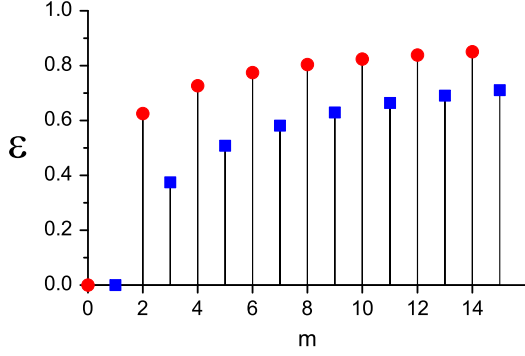


FIG. 5: (Color online) Measure of entanglement \mathcal{E} of the lowest states ($n_{c.m.} = n_z^{c.m.} = m_{c.m.} = 0, n = n_z = 0$) for various m in the limit of noninteracting electrons.

V. THE CONNECTION BETWEEN REPRESENTATIONS

As already mentioned, due to the separation (12), the eigenstates of the Hamiltonian H have a simpler form in the CM representation than in the IP one. However, the simplicity of this form holds back information on the inherent correlations of the two-electron orbital eigenfunctions $\psi(\mathbf{r}_1, \mathbf{r}_2)$. To illuminate this structure, one has to employ the IP representation.

The transition to the IP representation can be done by means of the expansion that holds for $m_{c.m.}, m \geq 0$ (see Appendix D)

$$\Phi_{0,m_{c.m.}}^{(c.m.)}(\mathbf{R})\Phi_{0,m}^{(\text{rel})}(\mathbf{r}_{12}) = \sum_{j=0}^{m_{c.m.}} \sum_{k=0}^m A_{j,k}^{m_{c.m.},m} \Phi_{0,M-j-k}(\mathbf{r}_1)\Phi_{0,j+k}(\mathbf{r}_2), \quad (47)$$

where $M = m_{c.m.} + m$, and

$$A_{j,k}^{m_{c.m.},m} = (-1)^k \binom{m_{c.m.}}{j} \binom{m}{k} \sqrt{\frac{(M-j-k)!(j+k)!}{2^M m_{c.m.}! m!}}, \quad (48)$$

combined with the identity $\phi_0^{(c.m.)}(Z)\phi_0^{(\text{rel})}(z_{12}) = \phi_0(z_1)\phi_0(z_2)$ (in the 3D case). Evidently, at $n_z^{c.m.} = n_z = 0$ the z -component of the orbital function does not contribute to the entanglement of the full state. Therefore, without loss of generality, we can use the 2D model.

If we set $m_{c.m.} = 0$ in Eqs. (47), (48) ($\Rightarrow j = 0$ and $m = M$), the following result is obtained for the states (43) (the 2D model) in the IP representation

$$\begin{aligned} \psi(\mathbf{r}_1, \mathbf{r}_2) &= \Phi_{0,0}^{(c.m.)}(\mathbf{R})\Phi_{0,0}^{(\text{rel})}(\mathbf{r}_{12}) \\ &= \sum_{k=0}^m A_{0,k}^{0,m} \Phi_{0,m-k}(\mathbf{r}_1)\Phi_{0,k}(\mathbf{r}_2). \end{aligned} \quad (49)$$

At $m = 0$, one has $\psi(\mathbf{r}_1, \mathbf{r}_2) = \Phi_{0,0}(\mathbf{r}_1)\Phi_{0,0}(\mathbf{r}_2)$, i.e., the orbital wave function can be written in the form of

the product of wave functions for individual electrons. Since the corresponding spin state ($S = M_S = 0$) is antisymmetric, the total wave function has the form of the Slater determinant. Thus, the entanglement of the lowest state with $m = 0$ must be zero.

At $m = 1$, by means of Eq. (49) we obtain the antisymmetric function

$$\psi(\mathbf{r}_1, \mathbf{r}_2) = \frac{1}{\sqrt{2}}[\Phi_{0,1}(\mathbf{r}_1)\Phi_{0,0}(\mathbf{r}_2) - \Phi_{0,0}(\mathbf{r}_1)\Phi_{0,1}(\mathbf{r}_2)]. \quad (50)$$

The corresponding spin state ($S = M_S = 1$) is the product of individual electron spin states with $m_s = +1/2$. Evidently, the total wave function is the Slater determinant, and its entanglement is zero.

At $m \geq 2$ the expansion (49) contains more than two terms. The two-electron orbital states are nontrivially correlated, i.e., cannot be reduced to the Slater determinant. The increase of the magnetic quantum number m increases the number of states in the decomposition (49). Evidently, it leads to more entangled states. Finally, the entanglement becomes maximal ($\mathcal{E} \rightarrow 1$) in the limit $m \rightarrow \infty$.

The transformation formula (47) demonstrates that all eigenstates of the Hamiltonian H (including those with $m_{c.m.} > 0$), that in the limit $V_C \rightarrow 0$ converge to the eigenstates of the noninteracting Hamiltonian H_0 with $n_1 = n_2 = 0$, can be written in the form of the product $\Phi_{0,m_{c.m.}}^{(c.m.)}(\mathbf{R})\Phi_{0,m}^{(\text{rel})}(\mathbf{r}_{12})$ in the same limit (see Table III). Since $j + k = m_2$ (and $M - m_2 = m_1$), we have

$$\begin{aligned} \Phi_{0,m_{c.m.}}^{(c.m.)}(\mathbf{R})\Phi_{0,m}^{(\text{rel})}(\mathbf{r}_{12}) &= \sum_{j=0}^{m_{c.m.}} \sum_{m_2=j}^{j+m} A_{j,m_2-j}^{m_{c.m.},m} \Phi_{0,M-m_2}(\mathbf{r}_1)\Phi_{0,m_2}(\mathbf{r}_2). \end{aligned} \quad (51)$$

By changing the summation order, we obtain

$$\begin{aligned} \Phi_{0,m_{c.m.}}^{(c.m.)}(\mathbf{R})\Phi_{0,m}^{(\text{rel})}(\mathbf{r}_{12}) &= \sum_{m_2=0}^M \sum_{j=\max(0,m_2-m)}^{\min(m_2,m_{c.m.})} A_{j,m_2-j}^{m_{c.m.},m} \Phi_{0,M-m_2}(\mathbf{r}_1)\Phi_{0,m_2}(\mathbf{r}_2). \end{aligned} \quad (52)$$

Comparing this latest relation with Eq. (34), one obtains

$$a_{m_2}^{(-1)^m} = \sum_{j=\max(0,m_2-m)}^{\min(m_2,m_{c.m.})} A_{j,m_2-j}^{m_{c.m.},m}. \quad (53)$$

With the aid of this relation and Eqs.(48), (38), we determine the trace of the square of the reduced density matrix (orbital part) and the measure \mathcal{E} for any $m_{c.m.}, m \geq 0$. Results for $m_{c.m.}, m = 0, 1, 2, 3$ are shown in Table III. In particular, for $m_{c.m.} = 0$ (then $j = 0, k = m_2$ and $M = m$) one has $a_{m_2}^{(-1)^m} = A_{0,m_2}^{0,m}$ and

$$\begin{aligned} \text{Tr}[\rho_r^{(\text{orb})}{}^2] &= \sum_{k=0}^m |A_{0,k}^{0,m}|^4 = \sum_{k=0}^m \binom{m}{k}^4 \left[\frac{(m-k)! k!}{2^m m!} \right]^2 \\ &= \frac{(2m)!}{(2^m m!)^2}. \end{aligned} \quad (54)$$

TABLE III: Individual particle and CM representations of the orbital parts of lowest states (including those with $m_{c.m.} > 0$) of axially symmetric two-electron QDs (in the magnetic field) in the limit of noninteracting electrons ($V_C \rightarrow 0$) for $M = 0, 1, 2, 3$, the related spin states (S, M_S), the traces of squares of the corresponding reduced density matrices and the values of the entanglement measure \mathcal{E} . The state, that is the lowest for a given M , corresponds to $m_{c.m.} = 0$ (shown on the top of each M -manifold) and $M_S = S$. The related values of \mathcal{E} (highlighted) coincide with those given in Table II.

M	orb. state	ind. particle rep.	CM rep.	$\text{Tr}[\rho_r^{(\text{orb})}{}^2]$	S	M_S	$\text{Tr}[\rho_r^{(\text{spin})}{}^2]$	\mathcal{E}
0	$\psi^{(0,+)}$	$u_1^{(0,+)}(\mathbf{r}_1, \mathbf{r}_2)$	$\Phi_{0,0}^{(c.m.)}(\mathbf{R})\Phi_{0,0}^{(\text{rel})}(\mathbf{r}_{12})$	1	0	0	1/2	0
1	$\psi^{(1,-)}$	$u_1^{(1,-)}(\mathbf{r}_1, \mathbf{r}_2)$	$\Phi_{0,0}^{(c.m.)}(\mathbf{R})\Phi_{0,1}^{(\text{rel})}(\mathbf{r}_{12})$	1/2	1	$0, \pm 1$	1/2, 1	1/2, 0
	$\psi^{(1,+)}$	$u_1^{(1,+)}(\mathbf{r}_1, \mathbf{r}_2)$	$\Phi_{0,1}^{(c.m.)}(\mathbf{R})\Phi_{0,0}^{(\text{rel})}(\mathbf{r}_{12})$	1/2	0	0	1/2	1/2
2	$\psi_{<}^{(2,+)}$	$\frac{1}{\sqrt{2}}[u_1^{(2,+)}(\mathbf{r}_1, \mathbf{r}_2) - u_2^{(2,+)}(\mathbf{r}_1, \mathbf{r}_2)]$	$\Phi_{0,0}^{(c.m.)}(\mathbf{R})\Phi_{0,2}^{(\text{rel})}(\mathbf{r}_{12})$	3/8	0	0	1/2	5/8
	$\psi^{(2,-)}$	$u_1^{(2,-)}(\mathbf{r}_1, \mathbf{r}_2)$	$\Phi_{0,1}^{(c.m.)}(\mathbf{R})\Phi_{0,1}^{(\text{rel})}(\mathbf{r}_{12})$	1/2	1	$0, \pm 1$	1/2, 1	1/2, 0
	$\psi_{>}^{(2,+)}$	$\frac{1}{\sqrt{2}}[u_1^{(2,+)}(\mathbf{r}_1, \mathbf{r}_2) + u_2^{(2,+)}(\mathbf{r}_1, \mathbf{r}_2)]$	$\Phi_{0,2}^{(c.m.)}(\mathbf{R})\Phi_{0,0}^{(\text{rel})}(\mathbf{r}_{12})$	3/8	0	0	1/2	5/8
3	$\psi_{<}^{(3,-)}$	$\frac{1}{2}[u_1^{(3,-)}(\mathbf{r}_1, \mathbf{r}_2) - \sqrt{3}u_2^{(3,-)}(\mathbf{r}_1, \mathbf{r}_2)]$	$\Phi_{0,0}^{(c.m.)}(\mathbf{R})\Phi_{0,3}^{(\text{rel})}(\mathbf{r}_{12})$	5/16	1	$0, \pm 1$	1/2, 1	11/16, 3/8
	$\psi_{<}^{(3,+)}$	$\frac{1}{2}[\sqrt{3}u_1^{(3,+)}(\mathbf{r}_1, \mathbf{r}_2) - u_2^{(3,+)}(\mathbf{r}_1, \mathbf{r}_2)]$	$\Phi_{0,1}^{(c.m.)}(\mathbf{R})\Phi_{0,2}^{(\text{rel})}(\mathbf{r}_{12})$	5/16	0	0	1/2	11/16
	$\psi_{>}^{(3,-)}$	$\frac{1}{2}[\sqrt{3}u_1^{(3,-)}(\mathbf{r}_1, \mathbf{r}_2) + u_2^{(3,-)}(\mathbf{r}_1, \mathbf{r}_2)]$	$\Phi_{0,2}^{(c.m.)}(\mathbf{R})\Phi_{0,1}^{(\text{rel})}(\mathbf{r}_{12})$	5/16	1	$0, \pm 1$	1/2, 1	11/16, 3/8
	$\psi_{>}^{(3,+)}$	$\frac{1}{2}[u_1^{(3,+)}(\mathbf{r}_1, \mathbf{r}_2) + \sqrt{3}u_2^{(3,+)}(\mathbf{r}_1, \mathbf{r}_2)]$	$\Phi_{0,3}^{(c.m.)}(\mathbf{R})\Phi_{0,0}^{(\text{rel})}(\mathbf{r}_{12})$	5/16	0	0	1/2	11/16

This expression and Eq. (40) lead to the formula (45) for the lowest states with $m_{c.m.} = 0$ and a given m .

The transition from the IP to the CM representation can be done by the inverse transformation of Eq. (47). For $n_1 = n_2 = 0$ and $m_1, m_2 \geq 0$ one has (see Appendix D)

$$\Phi_{0,m_1}(\mathbf{r}_1)\Phi_{0,m_2}(\mathbf{r}_2) = \sum_{j=0}^{m_1} \sum_{k=0}^{m_2} A_{j,k}^{m_1,m_2} \Phi_{0,M-j-k}^{(c.m.)}(\mathbf{R})\Phi_{0,j+k}^{(\text{rel})}(\mathbf{r}_{12}), \quad (55)$$

where the coefficients $A_{j,k}^{m_1,m_2}$ are given by Eq. (48), after replacing $m_{c.m.} \rightarrow m_1, m \rightarrow m_2$. For example, at $m_1 = m_2 = 1$, one obtains

$$u_2^{(2,+)}(\mathbf{r}_1, \mathbf{r}_2) \equiv \Phi_{0,1}(\mathbf{r}_1)\Phi_{0,1}(\mathbf{r}_2) = \frac{1}{\sqrt{2}}[\Phi_{0,2}^{(c.m.)}(\mathbf{R})\Phi_{0,0}^{(\text{rel})}(\mathbf{r}_{12}) - \Phi_{0,0}^{(c.m.)}(\mathbf{R})\Phi_{0,2}^{(\text{rel})}(\mathbf{r}_{12})]. \quad (56)$$

This expansion clearly demonstrates that, although the CM basis functions formally include correlations between particles (in contrast to the IP basis functions), non-entangled states (as well as entangled) states (such as $u_2^{(2,+)}$) can be regularly represented in this basis.

Regarding the last remarks, we point out that an analysis, if performed strictly in the CM representation, may lead in some cases to incorrect conclusions. An example is the analysis of the role of the inter-particle interaction in preparing entangled states. Namely, the form of the lowest states in the IP representation is non-trivially determined by the electron-electron interaction $V_C = \lambda/r_{12}$, even in the limit $\lambda \rightarrow 0$. In this limit the values of coefficients in the superposition (19) are specified (see Sec. III). Since the coefficients are not arbitrary

(in contrast to the case of the exact $\lambda = 0$), the states are entangled (see Table III). In the CM representation, however, the same states are simply the eigenstates of H_0 with specified (c.m.) symmetries. These symmetries exist regardless of whether the interaction V_C is present or not (due to decoupling of the c.m. and relative motions). Thus, in this representation the eigenstates of H (in the limit $V_C \rightarrow 0$) and H_0 are the same. One might conclude that the interaction V_C is not necessary to prepare an entangled state. Thus, we have obtained two opposite conclusions by analyzing the same effect in different representations.

The solution of this paradox lies in the fact that in the limit $V_C \rightarrow 0$ the form of interaction V_C is not crucial – the only requirement is that it must be a function of the relative distance \mathbf{r}_{12} only (i.e., it must be independent of \mathbf{R}) in order to keep the c.m. and relative motions decoupled. Then the interaction breaks only the symmetries of the noninteracting system, that are related to the integrals of motion of individual particles. This symmetry breaking removes the degeneracy (see the last paragraph in Sec. II B). It reduces the set of all eigenstates of H_0 to the subset of those that have symmetries related to the c.m. integrals of motion. Consequently, just this subset of eigenstates of H_0 is the complete set of eigenstates of H in the limit $V_C \rightarrow 0$. These states, although being the CM basis states, have the form of certain linear combinations of the IP basis states, i.e., they are entangled. The inter-particle interaction selects the eigenstates of a proper symmetry at the limit $\lambda \rightarrow 0$.

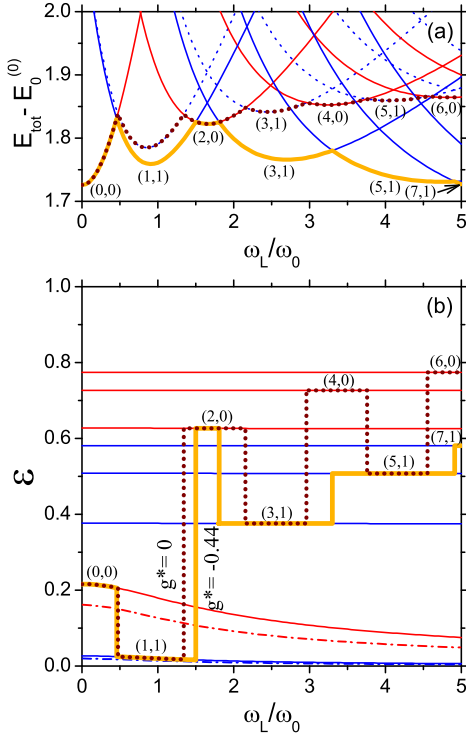


FIG. 6: (Color online) (a) Lowest energy levels (thin red and blue lines) and the ground state energy (thick lines) of axially symmetric two-electron QDs with $\lambda = 2$ (in $\hbar\omega_0\ell_0$ units) for $\omega_z/\omega_0 \gg 1$. In order to get a better resolution, the energies are defined with respect to the $E_0^{(0)}$ level (all energies are defined in $\hbar\omega_0$ units). The results for $g^* = 0$ and -0.44 are represented by dotted and solid lines, respectively. The numbers in parentheses are the values of quantum numbers (m, S) that characterize the corresponding states. b) Entanglement of the states corresponding to the levels shown in (a). Thick dotted and solid (orange) lines represent the entanglement of the ground state at $g^* = 0$ and -0.44 , respectively. Dash-dotted lines show the entanglement measure of the lowest levels with $M = 0$ and 1 obtained within the first-order approximation (see Eqs. (58), (63)).

VI. THE ENTANGLEMENT OF THE GROUND STATE IN THE MAGNETIC FIELD

At $V_C = 0$ the ground state orbital wave function with $m = 0$ is the product

$$\psi_{\text{gr}}^{(0)} = \Phi_{0,0}^{(c.m.)} \phi_0^{(c.m.)} \Phi_{0,0}^{(\text{rel})} \phi_0^{(\text{rel})} \quad (57)$$

(or $\Phi_{0,0}^{(c.m.)} \Phi_{0,0}^{(\text{rel})}$ within the 2D model). Among the states (43), it has the lowest energy at all values of the magnetic field.

The electron-electron interaction does not affect the c.m. motion. Therefore, even at $V_C \neq 0$, the ground state is characterized by $m_{c.m.} = 0$ for all values of the magnetic field B and the electron-electron interaction strength λ . The interaction leads, however, to the coupling (13) in ψ_{rel} . This results in the crossings of the

energy levels (as functions of B) with different values of the quantum number m [see Fig. 6(a)]. In addition, if we take into account the Zeeman splitting, for a negative Landé factor $g^* < 0$ the ground state spin quantum number of the m -th segment is determined by Eq. (39). According to this formula, the total spin $S = \frac{1}{2}[1 - (-1)^m]$ alternates between 0 and 1. This effect leads to the well known spin oscillations or singlet-triplet (ST) transitions in the ground state (see Refs. 8, 25 for a review).

As an example, the evolution of the ground state energy for two values of the Landé factor is shown on Fig. 6(a). A typical effect due to the Zeeman splitting is the dilation of the triplet state segments ($S = M_S = 1$) at the cost of the singlet ones ($S = 0$) with an increase of the magnetic field. The levels, that correspond to the singlet states, do not depend on g^* . The triplet states are lower for $g^* = -0.44$ than for $g^* = 0$. As a consequence, in the case $g^* = -0.44$ the segments $(m, S) = (0, 0)$ and especially $(2, 0)$ are reduced, and for $m > 2$ the singlet ground states are fully suppressed.

The measure \mathcal{E} , calculated for each ground state segment [Fig. 6(a)] separately, yields a discontinuous function $\mathcal{E}_{\text{gr}}(B)$ of the magnetic field [see Fig. 6(b)]. As we have seen in Fig. 5, the entanglement of the lowest state with $m = 0$ decreases by increasing the magnetic field. For the magnetic number $m \geq 2$ this dependence is, however, very weak [see Fig. 6(b)]. In fact, for these states the measure \mathcal{E} can be approximated by constant values that are close to the values (45) for the noninteracting case.

The Zeeman splitting does not affect the orbital wave function, and, therefore, the measure. However, different values of the Landé factor determine the position and length of (m, S) -segments [see Fig. 6(a)]. As a result, the variation of the measure $\mathcal{E}_{\text{gr}}(B)$ will be different for different values of g^* [see Fig. 6(b)].

By increasing the magnetic field, the ST transitions occur periodically at $g^* = 0$. Then, $\mathcal{E}_{\text{gr}}(B)$ is the combination [see Eq. (15)] of a "square-wave" function $\text{Tr}[\rho_r^{(\text{spin})2}]$ and a step function $\text{Tr}[\rho_r^{(\text{orb})2}]$. On the other hand, for $g^* = -0.44$ the ST transitions appear only a few times at lower values of the field. Finally, the system settles down in the triplet ground state with the quantum numbers $S = M_S = 1$. Consequently, the function $\mathcal{E}_{\text{gr}}(B)$ performs only a few oscillations in this case and, after that, it has the step function form.

Figure 7 shows the measure $\mathcal{E}(B)$ of the lowest states that contribute to the ground state, as well as $\mathcal{E}_{\text{gr}}(B)$, for two different values of the ratio ω_z/ω_0 and for $g^* = -0.44$. For larger values of the ratio ω_z/ω_0 the function $\mathcal{E}_{\text{gr}}(B)$ is similar to that obtained in the limit $\omega_z/\omega_0 \rightarrow \infty$ [shown in Fig. 6(b)]. By decreasing ω_z/ω_0 , the width of the peak related to the state $(2, 0)$ becomes smaller, and the positions of discontinuities are shifted to higher values of the magnetic field (see the results for $\omega_z/\omega_0 = 5$ in Fig. 7). At a sufficiently small value of the ratio ω_z/ω_0 the peak $(2, 0)$ disappears (see the case $\omega_z/\omega_0 = 2$ in

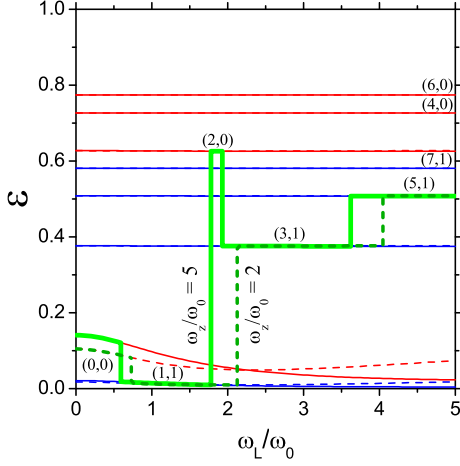


FIG. 7: (Color online) Entanglement of the lowest states with different m (thin red and blue lines) of axially symmetric two-electron QDs with $\lambda = 2$ (in $\hbar\omega_0\ell_0$ units), $g^* = -0.44$ and two values of the ratio ω_z/ω_0 equal 2 (dashed lines) and 5 (solid lines). The numbers in parentheses are the values of quantum numbers (m, S) which characterize the corresponding states. Entanglement of the ground state for these two cases is represented by the thick green line (dashed and solid, respectively).

Fig. 7). The function $\mathcal{E}_{\text{gr}}(B)$ has the step function form, except at the beginning [the segment (0,0)]. Evidently, the variation of this form with the change of the ratio ω_z/ω_0 is due to the shift of the ST-transition points [36], since for a given m the function $\mathcal{E}(B)$ does not change significantly.

VII. ESTIMATION OF THE ENTANGLEMENT FROM MEASURABLE QUANTITIES

From our analysis (Sec. IV) it follows that the entanglement of the lowest states with $m \geq 2$ depends only weakly on the strength of the Coulomb interaction λ (see Fig. 3). It is also found that the entanglement of these states is weakly dependent on the ratio ω_z/ω_0 , and on the magnetic field strength (see Fig. 4). These results suggest that Eq. (45), that determines (exactly) the entanglement measure \mathcal{E} of the lowest states in the limit $\lambda \rightarrow 0$, can be used as the zeroth-order approximation in the general case. In other words, formula (45) enables us to estimate the entanglement of the ground state of a QD with interacting electrons at the values of the magnetic field when $m \geq 2$. The only information required is just the value of the quantum number m (or M , because $m_{c.m.} = 0$). This feature is a consequence of the chosen (parabolic and axially symmetric) form of the confining potential. The magnetic quantum number M can be determined easily from the magnetic field dependence of the ground state energy and positions of the singlet-triplet transitions.

The zeroth-order approximation fails, however, if $M = 0$ or 1, since for these two values Eq. (45) gives $\mathcal{E} = 0$. The valuable results can be obtained within the first-order approximation, if we set $n_{\text{max}} = 1$ (and $n_z^{\text{max}} = 0$) in the expansion (41). As a result, we have

$$\mathcal{E} = 1 - \frac{3 - (-1)^m}{2} \left[I_0 b_0^4 + I_1 (4b_0^2 + b_1^2) b_1^2 \right]. \quad (58)$$

Here, for the sake of convenience, we introduce the notations: $I_0 = I(0, 0, 0, 0; m)$, $I_1 = I(0, 0, 1, 1; m) \equiv I(1, 1, 1, 1; m)$, and $b_n = b_{n,0}^{(m)}$. The values of I_0 are defined by Eq. (42), whereas $I_1 = 1/4, 3/16, 5/32, 35/256$ for $m = 0, 1, 2, 3$, respectively. To apply formula (58), in addition to the quantum number m , one needs to know also the coefficients b_0 and b_1 . These coefficients depend on the QD parameters and on the strength of the magnetic field (ω_0, λ and ω_L). Below we suggest how to estimate the coefficients b_0 and b_1 from the magnetic field dependence of the QD ground state energy.

Starting from the Hamiltonian for the relative motion (6) and applying the Hellmann-Feynman theorem, one obtains

$$\frac{\partial E_{\text{rel}}}{\partial \omega_L} = \mu \omega_L \langle \rho_{12}^2 \rangle - \langle l_z^{\text{rel}} \rangle. \quad (59)$$

Since we consider the QD in the ground state (with a given $M = m$), one has

$$\langle l_z^{\text{rel}} \rangle = \hbar m, \quad (60)$$

$$\langle \rho_{12}^2 \rangle \approx \frac{\hbar}{\mu \Omega} (m + 1 - 2b_0 b_1 \sqrt{m+1} + 2b_1^2), \quad (61)$$

where

$$b_0 \approx (1 - b_1^2)^{1/2} \quad (62)$$

(see Appendix E). As a result, Eq. (59) transforms to the form

$$\frac{\partial E_{\text{rel}}}{\partial \omega_L} \approx \hbar \frac{\omega_L}{\Omega} \left(m + 1 - 2\sqrt{m+1} \sqrt{b_1^2(1 - b_1^2) + 2b_1^2} \right) - \hbar m. \quad (63)$$

By means of elementary algebraic transformations, one obtains

$$(m + 2) b_1^4 + (F - m - 1) b_1^2 + F^2/4 = 0, \quad (64)$$

where

$$F(\omega_L) = 1 + \left(1 - \frac{\Omega}{\omega_L} \right) m - \frac{\Omega}{\omega_L} \frac{1}{\hbar} \frac{\partial E_{\text{rel}}}{\partial \omega_L}. \quad (65)$$

If at a given magnetic field strength B ($\sim \omega_L$) the values of the magnetic quantum number m and $\partial E_{\text{rel}}/\partial \omega_L$ are known, one can evaluate the expansion coefficients b_1 and b_0 with the aid of Eqs. (64), (62). By virtue of Eq. (58) it is straightforward to determine approximately the entanglement of the ground state of the QD at a given value of the magnetic field.

To illustrate the proposal we calculate the measure \mathcal{E} for the ground state energy as a function of the magnetic field, shown in Fig. 6(a). The obtained values of the measure \mathcal{E} for $M = 0$ and 1 reproduce qualitatively the exact dependence of the measure $\mathcal{E}(\omega_L)$, shown in Fig. 6(b) (the deviation is less than 30%). The results for the states $M \geq 2$ are in a remarkable agreement with exact values (in Fig. 6(b) they practically coincide). For example, at the value $\omega_L/\omega_0 = 1.65$ the ground state is characterized by $M = 2$ and $S = M_S = 0$. This value belongs to the narrow segment between the second and third ST transitions shown in Fig. 6. [This state is also marked in Figs. 1(b) and 2(b,c) by a red closed circle – the lower one.] Its entanglement measure is $\mathcal{E} = 0.6265$ (the exact value), whereas the values within the zeroth- and first-order approximation are $\mathcal{E}^{(0)} = 0.625$ and $\mathcal{E}^{(1)} = 0.6261$, respectively.

We point out that the relation (63) is crucial [together with Eq. (58)] for estimation of the entanglement of the QD ground state from experimental data. In fact, one has to know only the addition energy E_a for two-electron QDs

$$E_a = \mu(2) - \mu(1) = E_{\text{tot}}(2) - 2E_{\text{tot}}(1) \quad (66)$$

as a function of the magnetic field. Here $\mu(N) = E_{\text{tot}}(N) - E_{\text{tot}}(N-1)$ and $E_{\text{tot}}(N)$ are the chemical potential and the total ground state energy of the QD with N electrons, respectively. Thus, one has for one and two electrons

$$E_{\text{tot}}(1) = \hbar\Omega + \frac{\hbar\omega_z}{2} + g^* \mu_B B m_s, \quad (67)$$

$$E_{\text{tot}}(2) = E_{\text{rel}} + E_{\text{CM}} + g^* \mu_B B M_s, \quad (68)$$

where $E_{c.m.} = \hbar\Omega + \hbar\omega_z/2$. Assuming that in the one-electron ground state the spin projection $m_s = -1/2$, and applying the relation $\mu_B B = (m^*/m_e)\hbar\omega_L$, we obtain

$$E_a = E_{\text{rel}} - \left(\hbar\Omega + \frac{\hbar\omega_z}{2} \right) + g^* \frac{m^*}{m_e} \hbar\omega_L (M_s + 1). \quad (69)$$

As a result, the function $F(\omega_L)$ is expressed in terms of the derivative $\partial E_a / \partial \omega_L$

$$F = \left(1 - \frac{\Omega}{\omega_L} \right) m + \frac{\Omega}{\omega_L} \left[g^* \frac{m^*}{m_e} (M_s + 1) - \frac{1}{\hbar} \frac{\partial E_a}{\partial \omega_L} \right]. \quad (70)$$

If one knows the evolution of the addition energy E_a in the magnetic field, it becomes possible to evaluate $\partial E_a / \partial \omega_L$ at different values of ω_L and determine the function $F(\omega_L)$. Evidently, it will be a discontinuous function at those values of ω_L , where the ground state changes the (m, M_S) -values (singlet-triplet transitions). However, since $F(\omega_L)$ usually changes slowly in intervals between two transition points, it is sufficient to determine the value of F at an arbitrary point in each interval. It is particularly convenient if E_a has a local minimum at a ω_L -value inside the interval. At this point $\partial E_a / \partial \omega_L = 0$, and one needs to know only the corresponding value of

ω_L (or B) and the magnetic quantum number m to evaluate Eq. (70).

The proposed method is founded on the assumption that axially symmetric two-electron QDs can be approximated by the parabolic model. The ground state energy of the dot is calculated assuming that the dot is isolated. This approximation is well justified, when the tunneling between the QD and an external source and drain is relatively weak. We do not take into account the effect of finite temperature; this is appropriate for experiments which are performed at temperatures $k_B T \ll \hbar\omega_0$, with $\hbar\omega_0 \sim 2-5$ meV being the mean level spacing. Note that for these experiments a typical temperature is estimated to be below 100 mK (0.008 meV) [44, 45].

The analysis of numerous experimental data confirms that an effective trapping potential in small QDs with a few electrons is quite well approximated by a parabolic confinement [7, 9, 25]. Indeed, the validity of this approximation has been proven by the observation of the *shell structure* of a parabolic potential in small vertical quantum dots [44, 45], that was predicted theoretically in a number of publications [46–48]. Furthermore, a good agreement between experimental data and theoretical calculations of the addition energy has been demonstrated within the parabolic model as well (for a review see [25]). Taking into account the rapid development of the nano-sized technology and measurement techniques in the last decade we are very optimistic that our method could be useful to trace the entanglement properties in two-electron quantum dots in the magnetic field.

VIII. SUMMARY

We have considered a QD model that consists of two interacting electrons, confined in the axially-symmetric parabolic potential, in the external magnetic field. Within this model we have investigated in detail the connection between orbital correlations and the entanglement of the lowest two-electron states. These states compose a set of ground states at various values of the magnetic field.

We have analyzed integrals of motion and symmetries at zero and nonzero electron-electron interaction V_C . This analysis enabled us to introduce two appropriate basis sets: (i) the IP basis the elements of which are common eigenstates of the orbital part of the Hamiltonian with noninteracting electrons (H_0) and of the integrals of motion of individual electrons; (ii) the CM basis the elements of which are common eigenstates of the Hamiltonian H_0 and of the integrals of the c.m. and relative motions. To quantify the entanglement of two-electron states we have used the measure based on the linear entropy. With the aid of these representations we investigated how the orbital entanglement evolves at tuning of the interaction and the magnetic field strengths. For this purpose we have developed an analytical approach that enables to us to calculate the entanglement measure for

interacting and noninteracting electrons.

We have established the connection between the IP and CM representations of two-electron states, that allows us to readily illuminate quantum correlations. For example, in the limit of noninteracting electrons ($V_C \rightarrow 0$) in the CM representation the correlations between individual particles are hidden. Therefore, it is not quite evident whether a given state is entangled or not. To determine the entanglement one has either to calculate the entanglement measure, or to make a transition to the IP representation. We have shown that the elements of the CM basis are formally entangled (i.e., include interparticle correlations), even at zero interaction. This fact, however, does not imply that the stationary states of two non-interacting electrons are entangled. Due to the degeneracy of the energy levels at $V_C = 0$, one can always choose a set of eigenstates that exhibit a zero entanglement. Such a set is here the IP basis.

By means of our findings, we have studied the entanglement of the ground states of two-electron QDs in the magnetic field. It was demonstrated that at the magnetic quantum number $M \geq 2$ of the ground state the entanglement measure is remarkably well reproduced by means of analytical expressions obtained in the limit of noninteracting electrons $V_C \rightarrow 0$. Our analysis predicts a nonhomogeneous behavior of the entanglement as a function of the magnetic field. This feature arises due to singlet-triplet transitions. As soon as the singlet states are suppressed by the magnetic field, the entanglement is growing as a step function with an increase of the magnetic quantum number M .

By virtue of our analysis, we have proposed a practical approach to trace the evolution of the entanglement with the aid of the addition energy of two-electron QDs in the magnetic field. We hope that this approach would provide a practical method to measure the entangled states of QDs in the magnetic field.

Acknowledgments

This work was supported in part by RFBR Grant 14-02-00723 and by the Project 171020 of Ministry of Education and Science of Serbia. N.S.S. is grateful for the warm hospitality at UIB.

Appendix A: The individual particle basis

The IP basis elements are products of eigenstates of the Hamiltonians H_1 and H_2 . A favourable set of eigenstates of the single-electron Hamiltonians H_i ($i = 1, 2$) within the 2D model are the Fock-Darwin states $\Phi_{n_i, m_i}(\mathbf{r}_i)$, where $n_i = 0, 1, 2, \dots$ and $m_i = 0, \pm 1, \pm 2, \dots$ are the radial and magnetic quantum number of the electrons. The IP basis elements in the 2D model are, therefore, the products $\Phi_{n_1, m_1}(\mathbf{r}_1) \Phi_{n_2, m_2}(\mathbf{r}_2)$.

The Fock-Darwin states are stationary states of a charged particle, confined in an axially symmetric 2D parabolic potential, in a perpendicular magnetic field. Their explicit form is [40]

$$\Phi_{n_i, m_i}(\rho_i, \varphi_i) = \sqrt{\frac{\bar{\Omega}}{\pi}} \sqrt{\frac{n_i!}{(n_i + |m_i|)!}} (\sqrt{\bar{\Omega}} \rho_i)^{|m_i|} e^{-\frac{1}{2}\bar{\Omega} \rho_i^2} L_{n_i}^{|m_i|}(\bar{\Omega} \rho_i^2) e^{im_i \varphi_i}, \quad (\text{A1})$$

where $\rho_i = (x_i^2 + y_i^2)^{1/2}$, $\varphi_i = \arctan(y_i/x_i)$, $\bar{\Omega} = m^* \Omega / \hbar = (\Omega / \omega_0) / \ell_0^2$ and $L_{n_i}^{|m_i|}$ are the Laguerre polynomials. These states are simultaneously the eigenstates of $l_z^{(i)}$. The parity of the states is $(-1)^{m_i}$ and the corresponding (Fock-Darwin) energies are

$$E_{n_i, m_i} = \hbar \Omega (2n_i + |m_i| + 1) - \hbar \omega_L m_i. \quad (\text{A2})$$

A set of eigenstates of the single-electron Hamiltonians H_i ($i = 1, 2$) in the 3D model are the products $\Phi_{n_i, m_i}(\rho_i, \varphi_i) \phi_{n_{z_i}}(z_i)$, where

$$\phi_{n_{z_i}}(z_i) = \frac{(\bar{\omega}_z / \pi)^{1/4}}{\sqrt{2^{n_{z_i}} n_{z_i}!}} e^{-\frac{1}{2}\bar{\omega}_z z_i^2} H_{n_{z_i}}(\sqrt{\bar{\omega}_z} z_i), \quad (\text{A3})$$

are the eigenfunctions of the harmonic oscillator in the z -direction. Here $\bar{\omega}_z = m^* \omega_z / \hbar = 1 / \ell_z^2$, and $H_{n_{z_i}}$ are the Hermite polynomials ($n_{z_i} = 0, 1, 2, \dots$). The parity of the states $\Phi_{n_i, m_i}(\rho_i, \varphi_i) \phi_{n_{z_i}}(z_i)$ is $(-1)^{m_i + n_{z_i}}$. The related energy levels are

$$E_{n_i, m_i, n_{z_i}} = E_{n_i, m_i} + \hbar \omega_z (n_{z_i} + \frac{1}{2}). \quad (\text{A4})$$

Therefore, the IP basis elements in the 3D model are the products $\Phi_{n_1, m_1}(\mathbf{r}_1) \phi_{n_{z_1}}(z_1) \Phi_{n_2, m_2}(\mathbf{r}_2) \phi_{n_{z_2}}(z_2)$.

The (anti)symmetrized products of the Fock-Darwin states are defined as

$$\{\Phi_{n_1, m_1}(\mathbf{r}_1), \Phi_{n_2, m_2}(\mathbf{r}_2)\}_{\pm} \equiv A[\Phi_{n_1, m_1}(\mathbf{r}_1) \Phi_{n_2, m_2}(\mathbf{r}_2) \pm \Phi_{n_2, m_2}(\mathbf{r}_1) \Phi_{n_1, m_1}(\mathbf{r}_2)], \quad (\text{A5})$$

were $A = 1/2$ if $n_1 = n_2$ and $m_1 = m_2$, otherwise $A = 1/\sqrt{2}$. Note that $\{\Phi_{n_1, m_1}(\mathbf{r}_1), \Phi_{n_2, m_2}(\mathbf{r}_2)\}_- = 0$ if $n_1 = n_2$ and $m_1 = m_2$. The states (A5) are the elements of the (anti)symmetric counterparts of the IP basis in the 2D model. As the unsymmetrized states (A1), they are related to the eigenenergies (A2).

Appendix B: The center-of-mass basis

The CM basis elements are products of eigenstates of $H_{c.m.}$ and $H_{\text{rel}}^{(0)}$. These states have the same form as the single-electron states, but with the values $\mathcal{M} = 2m^*$ and $\mu = m^*/2$, respectively, instead of the effective electron mass m^* .

Therefore, the CM basis elements in the 2D model are the products $\Phi_{n_{c.m.}, m_{c.m.}}^{(c.m.)}(\mathbf{R}) \Phi_{n,m}^{(rel)}(\mathbf{r}_{12})$, where

$$\begin{aligned} \Phi_{n_{c.m.}, m_{c.m.}}^{(c.m.)}(\rho_{c.m.}, \varphi_{c.m.}) &= \sqrt{\frac{2\bar{\Omega}}{\pi}} \sqrt{\frac{n_{c.m.}!}{(n_{c.m.} + |m_{c.m.}|)!}} \\ &(\sqrt{2\bar{\Omega}} \rho_{c.m.})^{|m_{c.m.}|} e^{-\bar{\Omega}\rho_{c.m.}^2} L_{n_{c.m.}}^{|m_{c.m.}|}(2\bar{\Omega}\rho_{c.m.}^2) \times \\ &\times e^{im_{c.m.}\varphi_{c.m.}} \end{aligned} \quad (\text{B1})$$

and

$$\begin{aligned} \Phi_{n,m}^{(rel)}(\rho, \varphi) &= \sqrt{\frac{\bar{\Omega}}{2\pi}} \sqrt{\frac{n!}{(n+|m|)!}} \left(\sqrt{\frac{\bar{\Omega}}{2}} \rho\right)^{|m|} \\ &e^{-\frac{1}{4}\bar{\Omega}\rho^2} L_n^{|m|}(\bar{\Omega}\rho^2/2) e^{im\varphi}. \end{aligned} \quad (\text{B2})$$

Here $\rho_{c.m.} = (X^2 + Y^2)^{1/2}$, $\varphi_{c.m.} = \arctan(Y/X)$, $\rho = (x^2 + y^2)^{1/2}$ and $\varphi = \arctan(y/x)$. The labels $n_{c.m.}, n = 0, 1, 2, \dots$ and $m_{c.m.}, m = 0, \pm 1, \pm 2, \dots$ are the radial and magnetic quantum number of the c.m. and the relative motion degree of freedom, respectively. The states (B1) and (B2) are simultaneously the eigenstates of $l_z^{(c.m.)}$ and $l_z^{(rel)}$, respectively. The parities of these states are $(-1)^{m_{c.m.}}$ and $(-1)^m$, whereas the corresponding (Fock-Darwin) energies are

$$E_{n_{c.m.}, m_{c.m.}} = \hbar\Omega(2n_{c.m.} + |m_{c.m.}| + 1) - \hbar\omega_L m_{c.m.} \quad (\text{B3})$$

$$E_{n,m} = \hbar\Omega(2n + |m| + 1) - \hbar\omega_L m. \quad (\text{B4})$$

The CM basis elements in the 3D model are $\Phi_{n_{c.m.}, m_{c.m.}}^{(c.m.)}(\rho_{c.m.}, \varphi_{c.m.}) \phi_{n_z^{c.m.}}^{(c.m.)}(Z) \Phi_{n,m}^{(rel)}(\rho_{12}, \varphi_{12}) \phi_{n_z}^{(rel)}(z_{12})$, where

$$\phi_{n_z^{c.m.}}^{(c.m.)}(z_{c.m.}) = \frac{(2\bar{\omega}_z/\pi)^{1/4}}{\sqrt{2^{n_z^{c.m.}} n_z^{c.m.}!}} e^{-\bar{\omega}_z z_{c.m.}^2} \mathbf{H}_{n_z^{c.m.}}(\sqrt{2\bar{\omega}_z} z_{c.m.}) \quad (\text{B5})$$

and

$$\phi_{n_z}^{(rel)}(z) = \frac{(\bar{\omega}_z/2\pi)^{1/4}}{\sqrt{2^{n_z} n_z!}} e^{-\frac{1}{4}\bar{\omega}_z z^2} \mathbf{H}_{n_z}(\sqrt{\bar{\omega}_z/2} z), \quad (\text{B6})$$

$(n_z^{c.m.}, n_z = 0, 1, 2, \dots)$. The parities of the states $\Phi_{n_{c.m.}, m_{c.m.}}^{(c.m.)}(\rho_{c.m.}, \varphi_{c.m.}) \phi_{n_z^{c.m.}}^{(c.m.)}(Z)$ and $\Phi_{n,m}^{(rel)}(\rho, \varphi) \phi_{n_z}^{(rel)}(z)$ are $(-1)^{m_{c.m.} + n_z^{c.m.}}$ and $(-1)^{m + n_z}$, respectively. The related eigenenergies are

$$E_{n_{c.m.}, m_{c.m.}, n_z^{c.m.}} = E_{n_{c.m.}, m_{c.m.}} + \hbar\omega_z(n_z^{c.m.} + \frac{1}{2}) \quad (\text{B7})$$

$$E_{n,m,n_z} = E_{n,m} + \hbar\omega_z(n_z + \frac{1}{2}). \quad (\text{B8})$$

The CM basis functions have a definite exchange symmetry by construction. Indeed, the exchange of the particles 1 and 2 is equivalent to the transformation $\mathbf{r}_{12} \rightarrow -\mathbf{r}_{12}$ and the exchange symmetry of $\psi(\mathbf{r}_1, \mathbf{r}_2)$ is directly determined by the parity of $\psi_{rel}(\mathbf{r}_{12})$ and *vice versa*. Thus, the orbital wave function is symmetric (antisymmetric) if $\psi_{rel}(\mathbf{r}_{12})$ is even (odd). The c.m. coordinate \mathbf{R} is not affected by this transformation. As a

result, the wave function $\psi_{c.m.}$ does not change the sign by exchanging the particles. Therefore, if we construct the orbital wave function as the product (12), where the relative wave function is defined by (13) (with a fixed parity of the index n_z in the 3D case), the Pauli principle will be encountered automatically.

Appendix C: The I and J integrals

The I and J integrals appearing in the expansion (41) are

$$\begin{aligned} I(n_1, n_2, n_3, n_4; m) &= \int \cdots \int d\mathbf{r}_1 d\mathbf{r}'_1 d\mathbf{r}_2 d\mathbf{r}'_2 \times \\ &\Phi_{0,0}^{(c.m.)}\left(\frac{\mathbf{r}_1 + \mathbf{r}_2}{2}\right) \Phi_{0,0}^{(c.m.)*}\left(\frac{\mathbf{r}'_1 + \mathbf{r}'_2}{2}\right) \times \\ &\Phi_{0,0}^{(c.m.)*}\left(\frac{\mathbf{r}_1 + \mathbf{r}'_2}{2}\right) \Phi_{0,0}^{(c.m.)}\left(\frac{\mathbf{r}'_1 + \mathbf{r}_2}{2}\right) \times \\ &\Phi_{n_1, m}^{(rel)}(\mathbf{r}_1 - \mathbf{r}_2) \Phi_{n_2, m}^{(rel)*}(\mathbf{r}'_1 - \mathbf{r}_2) \times \\ &\Phi_{n_3, m}^{(rel)*}(\mathbf{r}_1 - \mathbf{r}'_2) \Phi_{n_4, m}^{(rel)}(\mathbf{r}'_1 - \mathbf{r}'_2) \end{aligned} \quad (\text{C1})$$

(here \mathbf{r}_i are vectors in the xy -plane) and

$$\begin{aligned} J(n_{z_1}, n_{z_2}, n_{z_3}, n_{z_4}) &= \int \cdots \int dz_1 dz'_1 dz_2 dz'_2 \times \\ &\phi_0^{(c.m.)}\left(\frac{z_1 + z_2}{2}\right) \phi_0^{(c.m.)*}\left(\frac{z'_1 + z'_2}{2}\right) \times \\ &\phi_0^{(c.m.)*}\left(\frac{z_1 + z'_2}{2}\right) \phi_0^{(c.m.)}\left(\frac{z'_1 + z_2}{2}\right) \times \\ &\phi_{n_{z_1}}^{(rel)}(z_1 - z_2) \phi_{n_{z_2}}^{(rel)*}(z'_1 - z_2) \times \\ &\phi_{n_{z_3}}^{(rel)*}(z_1 - z'_2) \phi_{n_{z_4}}^{(rel)}(z'_1 - z'_2). \end{aligned} \quad (\text{C2})$$

Using the expressions for the functions $\Phi_{n,m}^{(c.m.)}$ and $\phi_{n_z}^{(rel)}$ [Eqs. (A1) and (A3), where the parameters $\bar{\Omega}$ and $\bar{\omega}_z$ are replaced, respectively, by $2\bar{\Omega}$ and $2\bar{\omega}_z$ for the CM states and by $\bar{\Omega}/2$ and $\bar{\omega}_z/2$ for the relative motion states], one obtains the following explicit forms for these integrals

$$\begin{aligned} I(n_1, n_2, n_3, n_4; m) &= \frac{1}{\pi^4 4^{|m|}} \\ &\sqrt{\frac{n_1! n_2! n_3! n_4!}{(n_1 + |m|)! (n_2 + |m|)! (n_3 + |m|)! (n_4 + |m|)!}} \\ &\int \cdots \int dx_1 dy_1 dx'_1 dy'_1 dx_2 dy_2 dx'_2 dy'_2 \quad (\text{C3}) \\ &e^{-(x_1^2 + y_1^2 + x_1'^2 + y_1'^2 + x_2^2 + y_2^2 + x_2'^2 + y_2'^2)} \\ &[(x_1 - x_2) + i(y_1 - y_2)]^{|m|} [(x'_1 - x_2) - i(y'_1 - y_2)]^{|m|} \\ &[(x_1 - x'_2) - i(y_1 - y'_2)]^{|m|} [(x'_1 - x'_2) + i(y'_1 - y'_2)]^{|m|} \\ &L_{n_1}^{|m|}\left(\frac{(x_1 - x_2)^2 + (y_1 - y_2)^2}{2}\right) L_{n_2}^{|m|}\left(\frac{(x'_1 - x_2)^2 + (y'_1 - y_2)^2}{2}\right) \\ &L_{n_3}^{|m|}\left(\frac{(x_1 - x'_2)^2 + (y_1 - y'_2)^2}{2}\right) L_{n_4}^{|m|}\left(\frac{(x'_1 - x'_2)^2 + (y'_1 - y'_2)^2}{2}\right), \end{aligned}$$

$$\begin{aligned}
J(n_{z_1}, n_{z_2}, n_{z_3}, n_{z_4}) = & \\
& \frac{1}{\pi^2 \sqrt{2^{n_{z_1}+n_{z_2}+n_{z_3}+n_{z_4}} n_{z_1}! n_{z_2}! n_{z_3}! n_{z_4}!}} \\
& \int \cdots \int dz_1 dz_1' dz_2 dz_2' e^{-(z_1^2+z_1'^2+z_2^2+z_2'^2)} \quad (C4) \\
& H_{n_{z_1}}\left(\frac{z_1-z_2}{\sqrt{2}}\right) H_{n_{z_2}}\left(\frac{z_1'-z_2}{\sqrt{2}}\right) H_{n_{z_3}}\left(\frac{z_1-z_2'}{\sqrt{2}}\right) H_{n_{z_4}}\left(\frac{z_1'-z_2'}{\sqrt{2}}\right).
\end{aligned}$$

Evidently, the I and J integrals do not depend on the parameters $\bar{\Omega}$ and $\bar{\omega}_z$.

Some properties of the I and J integrals are

- (i) $I(n_1, n_2, n_3, n_4; m) = 0$ when $n_1 + n_4 \neq n_2 + n_3$;
- (ii) if (n'_1, n'_2, n'_3, n'_4) is a permutation of indices (n_1, n_2, n_3, n_4) such that $n_1 + n_4 = n_2 + n_3$ and $n'_1 + n'_4 = n'_2 + n'_3$, then $I(n'_1, n'_2, n'_3, n'_4; m) = I(n_1, n_2, n_3, n_4; m)$;
- (iii) $I(n_1, n_2, n_3, n_4; 0) = J^2(n_1, n_2, n_3, n_4)$.

Appendix D: Relations between the IP and CM basis elements

At $n_{c.m.} = n = 0$ and $m_{c.m.}, m \geq 0$, the product of the Fock-Darwin states for the c.m. and relative motions (given by Eqs. (B1) and (B2)) is

$$\begin{aligned}
\Phi_{0, m_{c.m.}}^{(c.m.)}(\mathbf{R}) \Phi_{0, m}^{(rel)}(\mathbf{r}_{12}) = & \\
& \sqrt{\frac{(2\bar{\Omega})^{m_{c.m.}+1}}{\pi m_{c.m.}!}} R^{m_{c.m.}} e^{-\bar{\Omega}R^2} e^{im_{c.m.}\varphi_{c.m.}} \times \\
& \sqrt{\frac{(\bar{\Omega}/2)^{m+1}}{\pi m!}} r_{12}^m e^{-\frac{1}{4}\bar{\Omega}r_{12}^2} e^{im\varphi_{12}} = \\
& \frac{\bar{\Omega}}{\pi} \sqrt{\frac{2^{m_{c.m.}-m} \bar{\Omega}^M}{m! m_{c.m.}!}} e^{-\bar{\Omega}(R^2+r_{12}^2/4)} \times \\
& (R e^{i\varphi_{c.m.}})^{m_{c.m.}} (r_{12} e^{i\varphi_{12}})^m, \quad (D1)
\end{aligned}$$

where $M = m_1 + m_2 = m_{c.m.} + m$. After the transition to the individual particle coordinates, applying the relation $2R^2 + r_{12}^2/2 = r_1^2 + r_2^2$ and the binomial expansions

$$\begin{aligned}
(R e^{i\varphi_{c.m.}})^{m_{c.m.}} = & \left(\frac{r_1 e^{i\varphi_1} + r_2 e^{i\varphi_2}}{2} \right)^{m_{c.m.}} = \\
& \frac{1}{2^{m_{c.m.}}} \sum_{j=0}^{m_{c.m.}} \binom{m_{c.m.}}{j} r_1^{m_{c.m.}-j} \times \\
& \times r_2^j e^{i(m_{c.m.}-j)\varphi_1} e^{ij\varphi_2}, \quad (D2)
\end{aligned}$$

taking into account

$$\begin{aligned}
(r_{12} e^{i\varphi_{12}})^m = & (r_1 e^{i\varphi_1} - r_2 e^{i\varphi_2})^m = \\
& \sum_{k=0}^m \binom{m}{k} r_1^{m-k} r_2^k e^{i(m-k)\varphi_2} e^{ik\varphi_1}, \quad (D3)
\end{aligned}$$

the product (D1) transforms to

$$\begin{aligned}
\Phi_{0, m_{c.m.}}^{(c.m.)}(\mathbf{R}) \Phi_{0, m}^{(rel)}(\mathbf{r}_{12}) = & \\
& \frac{\bar{\Omega}}{\pi} \frac{\bar{\Omega}^{M/2}}{\sqrt{2^M m_{c.m.}! m!}} e^{-\frac{1}{2}\bar{\Omega}(r_1^2+r_2^2)} \times \\
& \sum_{j=0}^{m_{c.m.}} \sum_{k=0}^m (-1)^k \binom{m_{c.m.}}{j} \binom{m}{k} r_1^{M-j-k} r_2^{j+k} \times \\
& e^{i(M-j-k)\varphi_1} e^{i(j+k)\varphi_2}. \quad (D4)
\end{aligned}$$

Applying, finally, the expression (A1) for the Fock-Darwin states, now for the individual particles, the product (D1) takes the form

$$\begin{aligned}
\Phi_{0, m_{c.m.}}^{(c.m.)}(\mathbf{R}) \Phi_{0, m}^{(rel)}(\mathbf{r}_{12}) = & \\
& \sum_{j=0}^{m_{c.m.}} \sum_{k=0}^m (-1)^k \binom{m_{c.m.}}{j} \binom{m}{k} \sqrt{\frac{(M-j-k)!(j+k)!}{2^M m_{c.m.}! m!}} \times \\
& \Phi_{0, M-j-k}(\mathbf{r}_1) \Phi_{0, j+k}(\mathbf{r}_2). \quad (D5)
\end{aligned}$$

Analogously we derive the inverse transformation

$$\begin{aligned}
\Phi_{0, m_1}(\mathbf{r}_1) \Phi_{0, m_2}(\mathbf{r}_2) = & \\
& \sum_{j=0}^{m_1} \sum_{k=0}^{m_2} (-1)^k \binom{m_1}{j} \binom{m_2}{k} \sqrt{\frac{(M-j-k)!(j+k)!}{2^M m_1! m_2!}} \times \\
& \Phi_{0, M-j-k}^{(c.m.)}(\mathbf{R}) \Phi_{0, j+k}^{(rel)}(\mathbf{r}_{12}). \quad (D6)
\end{aligned}$$

Appendix E: An approximate expression for $\langle \rho_{12}^2 \rangle$ in the ground state

The mean value of ρ_{12}^2 in an arbitrary state ψ_{rel} , given in the form of expansion (17), is

$$\langle \rho_{12}^2 \rangle = \sum_{n, n'} \sum_{n_z} b_{n, n_z}^{(m)*} b_{n', n_z}^{(m)} \langle n, m | \rho_{12}^2 | n', m \rangle. \quad (E1)$$

Here, the matrix elements

$$\begin{aligned}
\langle n, m | \rho_{12}^2 | n', m \rangle = & \frac{\hbar}{\mu\Omega} [(2n+m+1) \delta_{n, n'} - \\
& \sqrt{n(n+m)} \delta_{n-1, n'} - \\
& \sqrt{(n+1)(n+m+1)} \delta_{n+1, n'}] \quad (E2)
\end{aligned}$$

are calculated between the Fock-Darwin states $\Phi_{n, m}^{(rel)}$. The Kronecker symbols cancel the sum via n' , and, as result, one has

$$\begin{aligned}
\langle \rho_{12}^2 \rangle = & \frac{\hbar}{\mu\Omega} \sum_{n, n_z} [|b_{n, n_z}^{(m)}|^2 (2n+m+1) - \\
& (b_{n+1, n_z}^{(m)*} b_{n, n_z}^{(m)} + b_{n, n_z}^{(m)*} b_{n+1, n_z}^{(m)}) \times \\
& \sqrt{(n+1)(n+m+1)}]. \quad (E3)
\end{aligned}$$

For a typical two-electron QD in the ground state, the relation $|b_{0,0}^{(m)}| \gg |b_{1,0}^{(m)}| \gg |b_{0,1}^{(m)}|, |b_{2,0}^{(m)}|, \dots$ holds. Keeping only the terms with $b_{0,0}^{(m)}$ and $b_{1,0}^{(m)}$ and assuming that $|b_{0,0}^{(m)}|^2 + |b_{1,0}^{(m)}|^2 \approx 1$, the general expression (E3) is reduced to the form

$$\langle \rho_{12}^2 \rangle = \frac{\hbar}{\mu\Omega} \left[m + 1 + 2|b_{1,0}^{(m)}|^2 - (b_{1,0}^{(m)*} b_{0,0}^{(m)} + b_{0,0}^{(m)*} b_{1,0}^{(m)})\sqrt{m+1} \right]. \quad (\text{E4})$$

Finally, since the b -coefficients in the expansion of ψ_{rel} with a fixed value of m can always be chosen to be real, one obtains

$$\langle \rho_{12}^2 \rangle = \frac{\hbar}{\mu\Omega} \left[m + 1 - 2b_{0,0}^{(m)}b_{1,0}^{(m)}\sqrt{m+1} + 2b_{1,0}^{(m)2} \right]. \quad (\text{E5})$$

-
- [1] N. Nielsen and I. L. Chuang, *Quantum Computation and Quantum Information* (Cambridge University Press, Cambridge 2000).
- [2] I. Bengtsson and K. Zyczkowski, *Geometry of Quantum States: An Introduction to Quantum Entanglement* (Cambridge University Press, Cambridge, 2006).
- [3] S.M. Barnett, *Quantum Information* (Oxford University Press, New York, 2009).
- [4] L. Amico, R. Fazio, A. Osterloh, and V. Vedral, *Rev. Mod. Phys.* **80**, 517 (2008).
- [5] M. Tichy, F. Mintert, and A. Buchleitner, *J. Phys. B: At. Mol. Opt. Phys.* **44** 192001 (2011).
- [6] I. Buluta, S. Ashhab, and F. Nori, *Rep. Prog. Phys.* **74**, 104401 (2011).
- [7] S.M. Reimann and M. Manninen, *Rev. Mod. Phys.* **74**, 1283 (2002).
- [8] R. G. Nazmitdinov, *Phys. Part. Nucl.* **40**, 71 (2009).
- [9] H. Saarikoski, S.M. Reimann, A. Harju, and M. Manninen, *Rev. Mod. Phys.* **82**, 2785 (2010).
- [10] D. Loss and D.P. DiVincenzo, *Phys. Rev. A* **57**, 120 (1998).
- [11] R. Hanson, L.P. Kouwenhoven, J.R. Petta, S. Tarucha, and L. M. K. Vandersypen, *Rev. Mod. Phys.* **79**, 1217 (2007).
- [12] W.B. Gao, A. Imamoglu, H. Bernien, and R. Hanson, *Nature Phot.* **9**, 363 (2015).
- [13] K. Eckert, J. Schlimann, D. Bruss, and M. Lewenstein, *Ann. Phys.* **299**, 88 (2002).
- [14] F. Buscemi, P. Bordone, and A. Bertoni, *Phys.Rev. A* **75**, 032301 (2007).
- [15] J. Naudts and T. Verhulst, *Phys.Rev. A* **75**, 062104 (2007).
- [16] C. Amovilli and N.H. March, *Phys. Rev. A* **69**, 054302 (2004).
- [17] J.S. Dehesa, T. Koga, R.J. Yañez, A.R. Plastino, and R.O. Esquivel, *J. Phys. B: At. Mol. Opt. Phys.* **45**, 015504 (2012).
- [18] G. Benenti, S. Siccardi, and G. Strini, *Eur. Phys. J. D* **67**, 1 (2013).
- [19] Y.-C. Lin, C.-Y. Lin, and Y.K. Ho, *Phys. Rev. A* **87**, 022316 (2013).
- [20] C.-Y. Lin and Y.K. Ho, *Few-Body Syst.* **55**, 1141 (2014).
- [21] P. Kościak and A. Okopińska, *Few-Body Syst.* **55**, 1151 (2014).
- [22] S. López-Rosa, R.O. Esquivel, A.R. Plastino, and J.S. Dehesa, *J. Phys. B: At. Mol. Opt. Phys.* **48**, 175002 (2015).
- [23] R. J Yañez, A. R. Plastino, and J. S. Dehesa, *Eur. Phys. J. D* **56**, 141 (2010).
- [24] R.G. Nazmitdinov and A.V. Chizhov, *Optics and Spectroscopy* **112**, 319 (2012).
- [25] J.L. Birman, R.G. Nazmitdinov, and V.I. Yukalov, *Phys. Rep.* **526**, 1 (2013).
- [26] J.P. Coe, A. Sudbery, and I. D' Amico, *Phys. Rev. B* **77**, 205122 (2008).
- [27] P. Kościak and H. Hassanabadi, *Few-Body Syst.* **52**, 189 (2012).
- [28] P. Kościak and A. Okopińska, *Phys. Lett. A* **374** 3841 (2010).
- [29] F.M. Pont, O. Osenda, J.H. Toloza, and P. Serra, *Phys. Rev. A* **81**, 042518 (2010).
- [30] S. Schröter, H. Friedrich, and J. Madroñero, *Phys. Rev. A* **87**, 042507 (2013).
- [31] P. Kościak, *Phys. Lett. A* **377**, 2393 (2013).
- [32] R.G. Nazmitdinov, N.S. Simonović, A. R. Plastino and A. V. Chizhov, *J. Phys. B: At. Mol. Opt. Phys.* **45**, 205503 (2012).
- [33] R.G. Nazmitdinov and N.S. Simonović, *JETP Lett.* **97**, 199 (2013).
- [34] N. S. Simonović and R. G. Nazmitdinov, *Phys.Rev. A* **78**, 032115 (2008).
- [35] W. Kohn, *Phys. Rev.* **123**, 1242 (1961).
- [36] R.G. Nazmitdinov, N. S. Simonović, and J.-M. Rost, *Phys.Rev. B* **65**, 155307 (2002).
- [37] N. S. Simonović and R. G. Nazmitdinov, *Phys.Rev. B* **67**, 041305(R) (2003).
- [38] P.-M. Zhang, L.-P. Zou, P.A. Horvathy, and G.W. Gibbons, *Ann.Phys.* **341**, 94 (2014).
- [39] L.D. Landau and E.M. Lifshitz, *Quantum Mechanics, Third Edition: Non-Relativistic Theory* (Butterworth-Heinemann, Oxford, 2003).
- [40] V. Fock, *Z. Phys.* **47**, 446 (1928); C.G. Darwin, *Proc.Cambridge Philos. Soc.* **27**, 86 (1930).
- [41] T. Chakraborty, *Quantum Dots* (Elsevier, Amsterdam, 1999).
- [42] A. P. Majtey, A. R. Plastino and J. S. Dehesa, *J. Phys. A: Math. Theor.* **45**, 115309 (2012).
- [43] A. Puente, L. Serra, and R. G. Nazmitdinov, *Phys. Rev. B* **69**, 125315 (2004).
- [44] L.P. Kouwenhoven, D.G. Austing, and S. Tarucha, *Rep. Progr. Phys.* **64**, 701 (2001).
- [45] Y. Nishi, Y. Tokura, J. Gupta, G. Austing, and S. Tarucha, *Phys. Rev. B* **75**, 121301(R) (2007) .
- [46] M. Macucci, K. Hess, and G.J. Iafrate, *Phys. Rev. B* **48**, 17354 (1993); *J. Appl. Phys.* **77**, 3267 (1995).
- [47] W.D. Heiss and R.G. Nazmitdinov, *Phys. Lett. A* **222**, 309 (1996).
- [48] A. Wojs, P. Hawrylak, S. Fafard, and L. Jacak, *Phys.*

Rev. B54, 5604 (1996).